Risk Measures for DC Pension Plan Decumulation

Peter A. Forsyth[a] Yuying Li[b]

February 21, 2025

Abstract

As the developed world replaces Defined Benefit (DB) pension plans with Defined Contribution (DC) plans, there is a need to develop decumulation strategies for DC plan holders. Optimal decumulation can be viewed as a problem in optimal stochastic control. Formulation as a control problem requires specification of an objective function, which in turn requires a definition of reward and risk. An intuitive specification of reward is the total withdrawals over the retirement period. Most retirees view risk as the possibility of running out of savings. This paper investigates several possible left tail risk measures, in conjunction with DC plan decumulation. The risk measures studied include (i) expected shortfall (ii) linear shortfall and (iii) probability of shortfall. We establish that, under certain assumptions, the set of optimal controls associated with all expected reward and expected shortfall Pareto efficient frontier curves is identical to the set of optimal controls for all expected reward and linear shortfall Pareto efficient frontier curves. Optimal efficient frontiers are determined computationally for each risk measure, based on a parametric market model. Robustness of these strategies is determined by testing the strategies out-of-sample using block bootstrapping of historical data.

Keywords: decumulation, stochastic control, risk
JEL codes: G11, G22
AMS codes: 91G, 65N06, 65N12, 35Q93

1 Introduction

Internationally, there is a growing movement to replace Defined Benefit (DB) pension plans with Defined Contribution (DC) plans. A study of the P7 countries[1] reveals that in terms of fraction of total pension assets, DC plans have increased from 37% in 2003 to 58% in 2023 (Thinking Ahead Institute, 2024). In terms of individual countries, Australia has 88% of pension assets in DC plans, while Japan has only 5% of pension assets in DC plans. In the Netherlands, all DB plans will transition to collective DC plans by 2028.[2] The trend towards DC plans seems inevitable, since corporations and governments no longer desire to take on the risk of providing the guarantees implicit in DB plans.

[a]David R. Cheriton School of Computer Science, University of Waterloo, Waterloo ON, Canada N2L 3G1, `paforsyt@uwaterloo.ca`

[b]David R. Cheriton School of Computer Science, University of Waterloo, Waterloo ON, Canada N2L 3G1, `yuying@uwaterloo.ca`

[1]Australia, Canada, Japan, Netherlands, Switzerland, UK, US

[2]"The End of the Dutch Defined Benefit Model A Steeper Euro Swap Curve Ahead," `https://www.pimco.com/eu/en/insights/the-end-of-the-dutch-defined-benefit-model-a-steeper-euro-swap-curve-ahead`

During the accumulation phase of a DC plan, the burden of deciding on an asset allocation usually is relegated to the investor. However, upon retirement, the DC plan holder is faced with an even bigger challenge. During the decumulation stage of a DC plan, the retiree must decide on a withdrawal schedule and an asset allocation. Surveys have revealed that retirees fear running out of savings more than death (Hill, 2016). Consequently, it seems clear that the retiree wants to to withdraw as much as possible, but avoid ruin. The decumulation problem has been termed "the nastiest, hardest problem in finance," by William Sharpe (Ritholz, 2017).

While it is often suggested that retirees purchase annuities to reduce the risk of depletion of savings, annuities are not popular with DC plan holders (Peijnenburg et al., 2016). MacDonald et al. (2013) suggest that avoidance of annuities may be entirely rational.[3] For example, in the North American context, true inflation protected annuities are virtually unobtainable.

An extensive study of decumulation strategies can be found in Bernhardt and Donnelly (2018). Some recent strategies which involve pooling longevity risk, such as a modern tontine (Fullmer, 2019; Weinert and Gründl, 2021; Forsyth et al., 2024) appear promising. However, these types of plans are still in their infancy.

The standard wealth management advice given to retirees is usually some variant of the ubiquitous *4% rule* (Bengen, 1994). This rule suggests that retirees should (i) invest in a portfolio of 50% bonds and 50% equities, rebalanced annually and (ii) withdraw 4% of the initial capital each year (adjusted for inflation). We can consider that this advice is given to a 65-year old retiree, who wants to be sure that he/she does not run out of savings if he/she lives to age 95.[4]

This advice is justified on the basis of historical rolling 30 year periods, using US data. A retiree following this advice would never have run out of savings over any of these rolling thirty year periods. Various adjustments to this rule have been suggested many times, see e.g. Guyton and Klinger (2006). However, both the advice and historical tests can be criticized. Rolling thirty-year periods obviously have very high correlations. Use of constant weight stock allocation is somewhat simplistic, as is use of a constant (in real terms) withdrawal rate. In fact Irlam (2014) used dynamic programming methods to conclude that deterministic (i.e. glide path) allocation strategies are sub-optimal.[5] More recently, Anarkulova et al. (2023) suggest that the safe withdrawal rate might be much lower than the the 4% rule. In contrast to rolling historical periods, Anarkulova et al. (2023) use block bootstrap resampling to test withdrawal strategies. We will also use bootstrap resampling to test our results in this paper.

Nevertheless, the *four per cent rule* has seen wide adoption since the original publication over thirty years ago, and can be regarded as the default advice.

Contrary to commonly held beliefs, it appears that retirees are somewhat flexible in annual spending. A survey in Bannerje (2021) indicates that retirees actually adjust their lifestyle (i.e. what are perceived as fixed expenses) to match their cash flows.

In fact, recent surveys indicate that, if anything, many retirees underspend on the basis of their financial assets (Rappaport, 2019; Ackerly et al., 2021). Browning et al. (2016) suggests that these assets are being held as a reserve against unexpected medical expenses. However, Canada has a comprehensive public health care system, yet Hamilton (2001) finds that senior Canadian couples 85 and older either save or give away about 25% of their income.

All these facts indicate that we should allow some flexibility in withdrawals from pension savings, in order to ameliorate sequence of return risk.

Perhaps the most rigorous approach to the decumulation problem is to formulate this as a problem in optimal stochastic control. The controls in this case, are (i) the asset allocation, i.e.

[3] See also *"When do you need insurance?"* `https://donezra.com/217-when-do-you-need-insurance/`

[4] The probability of a 65-year old Canadian male living to age 95 is about 0.13.

[5] A constant weight strategy is trivially deterministic.

the stock/bond split and (ii) the withdrawal amounts (real) per year, subject to maximum and minimum constraints.

Of course, the first task in formulating an optimal control problem is to specify the objective function. One possibility is to formulate the decumulation problem in terms of a utility function, combining the withdrawals and final portfolio value. However, it seems clear (from the popularity of the four per cent rule), that investors prefer to delineate the trade off between risk (running out of savings) and reward (maximizing withdrawals).

We will consider basically the same problem as formulated by Bengen (1994). As a result, the obvious measure of reward is the total of the withdrawals (inflation adjusted) over a 30 year period. However, the choice of risk measure is not so clear. Since retirees are primarily concerned with running out of savings, we should be focused on left tail measures of risk.

The objective of this paper is to carry out a thorough investigation of the following tail risk measures, in the context of decumulation, in terms of portfolio value at year 30:

- Expected shortfall, i.e., the mean of the worst α fraction of the outcomes. Typically $\alpha = .05$.
- Linear shortfall, i.e. weighting negative portfolio values linearly.
- Probability of final portfolio value being negative.

We first formalize the equivalence between expected withdrawal reward and expected shortfall risk (EW-ES) and expected withdrawal reward and linear shortfall risk (EW-LS) efficient frontiers. We further compare the efficient frontiers generated using all three risk measures above. We calibrate a parametric stochastic model for stocks and bonds based on almost a century of data. We solve the optimal control problem via dynamic programming using the parametric model. The controls are tested out-of-sample, using block bootstrap resampling of historical data (Politis and Romano, 1994; Cogneau and Zakalmouline, 2013; Dichtl et al., 2016; Anarkulova et al., 2022; 2023).

One of our main results is that, under certain conditions, the set of optimal controls associated with all expected reward and shortfall Pareto efficient frontier curves is identical to the set of optimal controls for all expected reward and linear shortfall Pareto efficient frontier curves. Consequently the essential difference between EW-ES and EW-LS is in the parameter which specifies tail-risk level. This parameter is an explicit wealth level target in EW-LS versus a probability level in EW-ES.

We conclude that Linear Shortfall is an excellent practical measure of tail risk. Linear Shortfall (LS) is (i) trivially time consistent (ii) weights shortfall[6] (iii) is close to optimal in terms of expected shortfall and probability of shortfall (iv) has an intuitive interpretation and (v) has robust performance in out of sample bootstrap resampling tests. Consequently, we recommend use of expected total withdrawals (as a measure of reward) and linear shortfall (LS) as a measure of risk in the context of studying decumulation strategies.

2 Problem Setting

Spending rules (such as the four per cent rule) are clearly popular with retirees. It is interesting to note the following quotation from (Anarkulova et al., 2023)

> *"Current retirement spending practices demonstrate a revealed preference for spending rules over annuitization, such that the efficacy of spending rules is an important issue. ... Obtaining reliable, quantitative evidence on the 4% rule and alternative withdrawal rates is of critical importance given their widespread use."*

[6] Being short \$100,000 is worse than being short \$1.

Due to its wide acceptance in wealth management, we consider the scenario discussed in (Bengen, 1994). We consider a 65-year old retiree who desires fixed minimum annual (real) cash flows over a 30 year time horizon. We also impose a cap on maximum withdrawals in any year. From the CPM2014 table from the Canadian Institute of Actuaries[7], the probability that a 65-year old Canadian male attains the age of 95 is about 0.13. However, use of a 30 year time horizon is considered a prudent test for having a low probability of running out of savings. In addition, observe that we will not mortality weight future cash flows, as is done when averaging over a population for pricing annuities. Mortality weighting does not seem to be a useful concept for an individual retiree.

Since we allow investing in risky assets, with a minimum cash withdrawals each year, it is possible to exhaust savings. In this case, we continue to withdraw cash from the portfolio, which is equivalent to borrowing cash. This debt accumulates at the borrowing rate. Essentially, we are assuming that the investor has other assets, e.g. real estate, which can be used as a hedge of last resort. In practice, accumulated debt due to exhausting savings could be funded using a reverse mortgage, with real estate as collateral (Pfeiffer et al., 2013).

Note that real estate is not fungible with financial assets, except as a last resort. This mental bucketing of assets is a common tenet of behavioral finance (Shefrin and Thaler, 1988). As far as the real estate is concerned, if investments perform well, or the retiree passes away early, then the real estate can be a bequest.

The fact that the portfolio can become negative, and the required cash flows can add to debt, means that any tail risk measure will penalize these states. Hence, the optimal stochastic control will find strategies which make these states as unlikely as possible.

2.1 Notation, Formulation

The investor has access to two funds: a stock index and a constant maturity bond index. At any instant in time t, let the *amount* invested in the stock index fund be denoted by $S_t \equiv S(t)$, and similarly the amount invested in the bond index is denoted by $B_t \equiv B(t)$. These amounts are real, i.e. inflation adjusted. The total (real) value of the portfolio W_t is then

$$W_t = S_t + B_t \ . \tag{2.1}$$

For any time dependent function $g(t)$, we use the notation

$$g(t^+) \equiv \lim_{\epsilon \to 0^+} g(t+\epsilon) \ \ ; \ \ g(t^-) \equiv \lim_{\epsilon \to 0^+} g(t-\epsilon) \ \ . \tag{2.2}$$

Consider a set of discrete withdrawal/rebalancing times $\mathcal{T}$,

$$\mathcal{T} = \{t_0 = 0 < t_1 < t_2 < \ldots < t_M = T\}, \tag{2.3}$$

where T is the investment horizon. For ease of notation, we assume that $t_i - t_{i-1} = \Delta t = T/M$ is constant.

At each rebalancing time $t_i, i = 0, \ldots, M-1$, the investor first (i) withdraws an amount of cash $\mathfrak{q}_i$ from the portfolio and then (ii) rebalances the portfolio. More precisely

$$W(t_i^+) \quad = \quad W(t_i^-) - \mathfrak{q}_i \ . \tag{2.4}$$

Denote the state of the system at each time by $\mathcal{X}(t), t \in [0,T]$. Informally, the state can be regarded as the information necessary to model the system from time t onwards (Powell, 2025).

[7] `www.cia-ica.ca/docs/default-source/2014/214013e.pdf`.

Let the rebalancing control $\mathfrak{p}(\mathcal{X}(t_i^-))$ be the fraction in stocks after withdrawals, then,

$$
\begin{aligned}
S(t_i^+) &= \mathfrak{p}_i(\mathcal{X}(t_i^-))W(t_i^+) \\
& \quad \mathfrak{p}_i(\mathcal{X}(t_i^-)) \equiv \mathfrak{p}(\mathcal{X}(t_i^-), t_i) \\
B(t_i^+) &= W(t_i^+) - S(t_i^+) \ .
\end{aligned} \tag{2.5}
$$

We can regard the amount withdrawn $\mathfrak{q}_i(\cdot)$ as an additional control i.e. $\mathfrak{q}_i(\mathcal{X}(t_i^-)) = \mathfrak{q}(\mathcal{X}(t_i^-), t_i)$. Note we make the implicit assumption that the optimal controls are of feedback form, i.e. only a function of the state and time.

Based on the parametric SDE model for (S_t,B_t) in Appendix A and Forsyth (2022), we will assume in the following that $\mathcal{X}(t) = (S(t), B(t)), t \in [0,T]$, with the realized state of the system denoted by $x = (s,b)$. More generally, of course, it may be necessary to include other variables to define the state (e.g. *lifting the state space* to include path dependent variables).[8]

In the special case that there are no transaction costs $\mathfrak{q}_i(\cdot) = \mathfrak{q}_i(W_i^-)$ and $\mathfrak{p}_i(\cdot) = \mathfrak{p}(W_i^+)$, i.e. the amount withdrawn is only a function of total wealth before withdrawals, and the rebalancing fraction is only a function of wealth after withdrawals. Note that it is straightforward to include transaction costs, but if typical costs for ETFs are included, this has a very small impact on the controls (Dang and Forsyth, 2014).

The control at time t_i is given by $(\mathfrak{q}_i(\cdot), \mathfrak{p}_i(\cdot))$, where $(\cdot)$ denotes the control as a function of state. We specify feasibility of control by prescribing the set of admissible *values* of the controls by $\mathcal{Z}$, i.e.,

$$
(\mathfrak{q}_i,\mathfrak{p}_i) \in \mathcal{Z}(W_i^-, W_i^+,t_i) = \mathcal{Z}_{\mathfrak{q}}(W_i^-, t_i) \times \mathcal{Z}_{\mathfrak{p}}(W_i^+,t_i) \ . \tag{2.6}
$$

where

$$
\mathcal{Z}_{\mathfrak{q}}(W_i^-, t_i) = \begin{cases} [\mathfrak{q}_{\min},\mathfrak{q}_{\max}] & t_i \in \mathcal{T} \ ; \ t_i \neq t_M \ ; \ W_i^- \geq \mathfrak{q}_{\max} \\ [\mathfrak{q}_{\min}, \max(\mathfrak{q}_{\min},W_i^-)] & t_i \in \mathcal{T} \ ; \ t \neq t_M \ ; \ W_i^- < \mathfrak{q}_{\max} \\ \{0\} & t_i = t_M \end{cases} , \tag{2.7}
$$

$$
\mathcal{Z}_{\mathfrak{p}}(W_i^+,t_i) = \begin{cases} [0,1] & W_i^+ > 0 \ ; \ t_i \in \mathcal{T} \ ; \ t_i \neq t_M \\ \{0\} & W_i^+ \leq 0 \ ; \ t_i \in \mathcal{T} \ ; \ t_i \neq t_M \\ \{0\} & t_i = t_M \end{cases} . \tag{2.8}
$$

These expressions encapsulate the following constraints:

- No shorting, no leverage (assuming solvency, i.e., when $W_i^+ > 0$),
- Maximum $\mathfrak{q}_{\max}$ and minimum $\mathfrak{q}_{\min}$ withdrawal constraints,
- In the case of insolvency $W_i^+ < 0$, trading ceases and debt accumulates at the borrowing rate,
- At $t = t_M$, all stocks are liquidated no withdrawals $\mathfrak{q}_M = 0$,
- If $W_i^- < \mathfrak{q}_{\max}$, the investor attempts to avoid insolvency, but always withdraws at least $\mathfrak{q}_{\min}$.

Recall that we assume that the retiree can finance the debt using other assets, e.g. a real estate hedge of last resort. At first sight it might seem appropriate to simply cease withdrawals if insolvent. However, by assumption, the retiree needs a minimum cash flow of $\mathfrak{q}_{\min}$ each year. Therefore, we

[8] A classic example is the pricing of an Asian option, which depends of the observed average stock price A_t. If the stock price S_t follows GBM, then the state space for an Asian option is lifted to (S_t, A_t).

penalize any set of controls which causes the retiree to exhaust his savings (and access the assumed real estate hedge) in order to fund the minimum cash flows. Allowing debt to accumulate also penalizes early insolvency compared to late insolvency.

The admissible control set $\mathcal{A}$ can then be written as

$$\mathcal{A} = \left\{ (\mathfrak{q}_i, \mathfrak{p}_i)_{0 \le i \le M} : (\mathfrak{p}_i, \mathfrak{q}_i) \in \mathcal{Z}(W_i^-, W_i^+, t_i) \right\} . \tag{2.9}$$

For notational simplicity, we denote a dynamic control by $\mathcal{P}$, and an admissible control $\mathcal{P} \in \mathcal{A}$ can be written as

$$\mathcal{P} = \{ (\mathfrak{q}_i(\cdot), \mathfrak{p}_i(\cdot)) \ : \ i = 0, \ldots, M \} . \tag{2.10}$$

We also define $\mathcal{P}_n \equiv \mathcal{P}_{t_n} \subset \mathcal{P}$ as the tail of the set of controls in $[t_n, t_{n+1}, \ldots, t_M]$, i.e.

$$\mathcal{P}_n = \{ (\mathfrak{q}_n(\cdot), \mathfrak{p}_n(\cdot)), \ldots, (\mathfrak{q}_M(\cdot), \mathfrak{p}_M(\cdot)) \} . \tag{2.11}$$

For notational completeness, we also define the tail of the admissible control set $\mathcal{A}_n$ as

$$\mathcal{A}_n = \left\{ (\mathfrak{q}_i, \mathfrak{p}_i)_{n \le i \le M} : (\mathfrak{q}_i, \mathfrak{p}_i) \in \mathcal{Z}(W_i^-, W_i^+, t_i) \right\} , \tag{2.12}$$

so that $\mathcal{P}_n \in \mathcal{A}_n$.

3 Risk and reward

3.1 Reward

Define $E_{\mathcal{P}_0}^{\mathcal{X}_0^-, t_0^-}[\cdot]$ as the expectation conditional on the observation at time t_0^-, state $\mathcal{X}_0^-$, under control $\mathcal{P}_0$. We then define reward as

$$\text{EW } (\mathcal{X}_0^-, t_0^-) \quad = \quad E_{\mathcal{P}_0}^{\mathcal{X}_0^-, t_0^-} \left[\sum_{i=0}^{M} \mathfrak{q}_i \right] \tag{3.1}$$

which is the total expected withdrawals in [0,T]. We will use EW as the reward measure in all cases. Note that $\mathfrak{q}_i$ is inflation adjusted and that we do not discount the future cash flows. We view this as a conservative approach and is consistent with the Bengen (1994) scenario.

3.2 Risk

PS We define PS risk as the probability of shortfall w.r.t. a terminal wealth level $\mathbb{W}$,

$$\text{PS}(\mathcal{X}_0^-, t_0^-) = Prob[W_T < \mathbb{W}] = E_{\mathcal{P}_0}^{\mathcal{X}_0^-, t_0^-} [\mathbf{1}_{W_T < \mathbb{W}}] . \tag{3.2}$$

Usually, $\mathbb{W}$ is zero, i.e., we are concerned with running out of cash. We want to *minimize* PS risk.

LS Linear shortfall

$$\text{LS}(\mathcal{X}_0^-, t_0^-) \quad = \quad E_{\mathcal{P}_0}^{\mathcal{X}_0^-, t_0^-} [\min(W_T - \mathbb{W}, 0)] . \tag{3.3}$$

Note that PS risk does not differentiate bad outcomes. Clearly, being short 1\$ is not as bad as being short 1000\$. LS weights the bad outcomes. Since ES is defined in terms of final wealth, not losses, we want to *maximize* LS risk measure.

Acronym	Description
EW (expected withdrawals)	$E[\sum_{i=0}^{M} \mathfrak{q}_i]$
PS (probability of shortfall)	$E[\mathbf{1}_{W_T<\mathbb{W}}]$
LS (linear shortfall)	$E[\min(W_T - \mathbb{W}, 0)]$
ES (expected shortfall)	$E\left[\frac{W_T \mathbf{1}_{W_T<\mathbb{W}}}{\alpha}\right]$
	s.t. $E[\mathbf{1}_{W_T<\mathbb{W}}] = \alpha$

TABLE 3.1: *Definition of acronyms.*

ES ES is the mean of the worst α fraction of outcomes. A common choice is $\alpha = .05$. More precisely, let W_T be the wealth associated with $\mathcal{P}_0{}^{\mathcal{X}_0^-, t_0^-}$

$$\mathrm{ES}(\mathcal{X}_0^-, t_0^-) = E_{\mathcal{P}_0}^{\mathcal{X}_0^-, t_0^-}\left[\frac{W_T \mathbf{1}_{W_T<\mathbb{W}}}{\alpha}\right] \quad \text{subject to } \left\{ E_{\mathcal{P}_0}^{\mathcal{X}_0^-, t_0^-}[\mathbf{1}_{W_T<\mathbb{W}}] = \alpha. \right. \tag{3.4}$$

We want to *maximize* ES risk measure.

One of the main goals of this paper is to compare and contrast these different reward-risk combinations, both mathematically and computationally.

3.3 Summary of Acronyms

For future reference, Table 3.1 lists the acronyms used in this paper.

4 Pareto points

We will use a scalarization technique to determine Pareto optimal points for the multi-objective problems balancing risk and reward. As an example consider problem EW-PS. Informally, given an scalarization parameter $\kappa > 0$, we seek the optimal control $\mathcal{P}_0$ that maximizes

$$\mathrm{EW}(\mathcal{X}_0^-, t_0^-) - \kappa\ \mathrm{PS}(\mathcal{X}_0^-, t_0^-)\ . \tag{4.1}$$

Varying κ traces out an efficient frontier in the (EW, PS) plane. For any fixed value of PS, the corresponding point on the efficient frontier is the largest possible value of EW.

4.1 PS, LS

We solve optimal control problem for weighted reward and risk combinations, e.g., EW-PS, EW-LS. To be precise, for each reward and risk parameter pair, we define the function $G(W_T, \mathbb{W})$ below,

$$\mathrm{PS} \ :\ G_{PS}(W_T, \mathbb{W}) = -\mathbf{1}_{W_T<\mathbb{W}} \tag{4.2}$$

$$\mathrm{LS} \ :\ G_{LS}(W_T, \mathbb{W}) = \min(W_T - \mathbb{W}, 0)\ , \tag{4.3}$$

where $\mathbb{W}$ is a specified wealth level. Assuming a risk aversion scaling parameter κ, the general problem for EW-xS, ($x = \{$P,L$\}$) can be written as

$$\text{EW-xS}_{t_0}\,(\mathbb{W},\kappa) : \sup_{\mathcal{P}_0\in\mathcal{A}} \left\{ E^{\mathcal{X}_0^+,t_0^+}_{\mathcal{P}_0}\left[\sum_{i=0}^{M} \mathfrak{q}_i + \kappa G_{\text{xS}}(W_T,\mathbb{W}) \right.\right.$$
$$\left.\left. + \,\epsilon W_T \middle| \mathcal{X}(t_0^-) = (s,b) \right] \right\} \tag{4.4}$$

$$\text{subject to} \begin{cases} (S_t, B_t) \text{ follow processes (A.3) and (A.4)}; \quad t \notin \mathcal{T} \\ W_\ell^+ = W_\ell^- - \mathfrak{q}_\ell\,;\ \mathcal{X}_\ell^+ = (S_\ell^+, B_\ell^+) \\ W_\ell^- = S(t_i^-) + B(t_i^-) \\ S_\ell^+ = \mathfrak{p}_\ell(\cdot)W_\ell^+\,;\ B_\ell^+ = (1-\mathfrak{p}_\ell(\cdot))W_\ell^+ \\ (\mathfrak{q}_\ell(\cdot),\mathfrak{p}_\ell(\cdot)) \in \mathcal{Z}(W_\ell^-, W_\ell^+, t_\ell) \\ \ell = 0,\ldots,M\ ;\ t_\ell \in \mathcal{T} \end{cases} . \tag{4.5}$$

Observe that we have added the stabilization term ϵW_T to the objective function in equation (4.4). The control problem is ill-posed in the cases where $t \to T, W_t \gg \mathbb{W}$. In this case, due to the maximum withdrawal constraint, and since the $Prob[W_t < \mathbb{W}] \simeq 0$, then the control has almost no effect on the objective function. Addition of the stabilization term regularizes the problem (see e.g. Chen et al. (2023)). We will discuss this further in later sections.

4.2 Expected Shortfall (ES)

We are interested in the relationship between the above reward-risk formulations with the same reward but ES risk, i.e.,

$$\text{EW}(\mathcal{X}_0^-, t_0^-) + \kappa\ \text{ES}(\mathcal{X}_0^-, t_0^-)\ . \tag{4.6}$$

We formulate the EW-ES optimal control problem using the technique in Rockafellar and Uryasev (2000), more precisely ($0 < \alpha < 1$)

$$\text{EW-ES}_{t_0}\,(\alpha,\kappa) : \sup_{\mathcal{P}_0\in\mathcal{A}} \left\{ E^{\mathcal{X}_0^-,t_0^-}_{\mathcal{P}_0}\left[\ \sum_{i=0}^{M} q_i\ +\ \kappa \sup_{W'} \left(W' + \frac{1}{\alpha}\min(W_T - W', 0) \right) \right.\right.$$
$$\left.\left. + \epsilon W_T \middle| (s,b) \right] \right\} \tag{4.7}$$
$$\text{subject to} \left\{ \text{Conditions (4.5)} \right. .$$

Interchanging the order in *sup sup*$\{\cdot\}$ in problem (4.7), we equivalently have

$$\text{EW-ES}_{t_0}\,(\alpha,\kappa) : \sup_{W'} \sup_{\mathcal{P}_0\in\mathcal{A}} \left\{ E^{\mathcal{X}_0^-,t_0^-}_{\mathcal{P}_0}\left[\ \sum_{i=0}^{M} q_i\ +\ \kappa \left(W' + \frac{1}{\alpha}\min(W_T - W', 0) \right) \right.\right.$$
$$\left.\left. + \epsilon W_T \middle| \mathcal{X}_0^- = (s,b) \right] \right\} \tag{4.8}$$
$$\text{subject to} \left\{ \text{Conditions (4.5)} \right. .$$

Note that, as for the EW-xS problems, we have added a stabilization term ϵW_T to the objective function.

Remark 4.1 (Pre-commitment policy)**.** *Note that the optimal control for problem (4.8) is formally a pre-commitment policy (Forsyth, 2020a). We delay further discussion concerning this issue to Section 4.4.*

4.3 Properties of optimal solution of EW-ES formulation (4.8)

Let $\mathcal{P}_0$ be any permissible control for problem (4.8) and W_T be the wealth corresponding to $\mathcal{P}_0$. Consider the maximizer below:[9]

$$\begin{aligned}\mathbb{W} \;&=\; \arg\max_{W'} \Bigg\{ E_{\mathcal{P}_0}^{\mathcal{X}_0^-, t_0^-} \Bigg[\sum_{i=0}^{M} q_i \;+\; \kappa \Big(W' + \frac{1}{\alpha} \min(W_T - W', 0) \Big) \\ &\qquad + \epsilon W_T \Bigg| \mathcal{X}_0^- = (s,b) \Bigg] \Bigg\} . \end{aligned} \tag{4.9}$$

Following Rockafellar and Uryasev (2000), it can be shown that (4.9) is equivalent to the probability constraint below, under the assumption of continuity in distribution of W_T,

$$E_{\mathcal{P}_0}^{\mathcal{X}_0^-, t_0^-} [\mathbf{1}_{W_T < \mathbb{W}}] \;=\; \alpha \; . \tag{4.10}$$

Let $E_{\mathcal{P}_0}$ denote $E_{\mathcal{P}_0}^{\mathcal{X}_0^-, t_0^-}$ for notational simplicity. Consider

$$\begin{aligned} & E_{\mathcal{P}_0} \Big(\mathbb{W} + \frac{1}{\alpha} \min(W_T - \mathbb{W}, 0) \Big) \\ & \text{subject to} \\ & \Big\{ E_{\mathcal{P}_0}[\mathbf{1}_{W_T \le \mathbb{W}}] = \alpha \quad . \end{aligned} \tag{4.11}$$

Let $g_{\mathcal{P}_0}(W_T)$ be the density of W_T under control $\mathcal{P}_0$. Then, write equation (4.11) as

$$\int_{-\infty}^{+\infty} \mathbb{W} \; g_{\mathcal{P}_0}(W_T) \; dW_T + \frac{1}{\alpha} \int_{-\infty}^{\mathbb{W}} (W_T - \mathbb{W}) \; g_{\mathcal{P}_0}(W_T) \; dW_T \tag{4.12}$$

$$\begin{aligned} & \text{subject to} \\ & \Big\{ \textstyle\int_{-\infty}^{\mathbb{W}} g_{\mathcal{P}_0}(W_T) \; dW_T = \alpha \quad . \end{aligned} \tag{4.13}$$

We can write (4.12) as

$$\mathbb{W} \int_{-\infty}^{+\infty} g_{\mathcal{P}_0}(W_T) \; dW_T - \frac{\mathbb{W}}{\alpha} \int_{-\infty}^{\mathbb{W}} G_{\mathcal{P}_0}(W_T) \; dW_T + \frac{1}{\alpha} \int_{-\infty}^{\mathbb{W}} W_T \; g_{\mathcal{P}_0}(W_T) \; dW_T \; . \tag{4.14}$$

Using equation (4.13), this becomes

$$\mathbb{W} - \mathbb{W} + \frac{1}{\alpha} \int_{-\infty}^{\mathbb{W}} W_T \; g_{\mathcal{P}_0}(W_T) \; dW_T \;=\; E_{\mathcal{P}_0}^{\mathcal{X}_0^-, t_0^-} \left[\frac{W_T \mathbf{1}_{W_T < \mathbb{W}}}{\alpha} \right] . \tag{4.15}$$

Thus, when (4.9) is satisfied, we have

$$\begin{aligned} E_{\mathcal{P}_0}^{\mathcal{X}_0^-, t_0^-} [\mathbf{1}_{W_T < \mathbb{W}}] \;&=\; \alpha \\ E_{\mathcal{P}_0}^{\mathcal{X}_0^-, t_0^-} \left[\frac{W_T \mathbf{1}_{W_T < \mathbb{W}}}{\alpha} \right] \;&=\; E_{\mathcal{P}_0}^{\mathcal{X}_0^-, t_0^-} \left[\Big(\mathbb{W} + \frac{1}{\alpha} \min(W_T - \mathbb{W}, 0) \Big) \right] . \end{aligned} \tag{4.16}$$

[9]The arg max is well defined since $\sup_{\mathcal{P}}\{\cdot\}$ is a continuous function of W'.

Consider the optimal $\mathbb{W}^*$ and control $\mathcal{P}_0^*$ from EW-ES$_{t_0}(\alpha,\kappa)$, equation (4.8), i.e.,

$$
\begin{aligned}
\mathbb{W}^* \;&=\; \arg\max_{W'} \sup_{\mathcal{P}_0 \in \mathcal{A}} \Bigg\{ E_{\mathcal{P}_0}^{\mathcal{X}_0^-, t_0^-} \Bigg[\sum_{i=0}^{M} q_i \;+\; \kappa \Big(W' + \frac{1}{\alpha} \min(W_T - W', 0) \Big) \\
&\qquad + \epsilon W_T \Bigg| \mathcal{X}_0^- = (s,b) \Bigg] \Bigg\} , \qquad (4.17)
\end{aligned}
$$

then equation (4.16) implies

$$
\begin{aligned}
Prob[W_T^* < \mathbb{W}^*] \;&=\; \alpha \qquad (4.18) \\
ES \;&=\; \text{mean of worst } \alpha \text{ fraction of outcomes} \\
&=\; E_{\mathcal{P}_0^*}^{\mathcal{X}_0^-, t_0^-} \Big[\Big(\mathbb{W}^* + \frac{1}{\alpha} \min(W_T^* - \mathbb{W}^*, 0) \Big) \Big] .
\end{aligned}
$$

From (4.18), we see immediately that $\mathbb{W}^*$ is the α-VaR (value at risk) of the terminal wealth W_T^* associated with the optimal control.

Fixing any target wealth level $\mathbb{W}$, we consider linear shortfall Pareto optimization ($\hat{\kappa} > 0$):

$$
\begin{aligned}
\text{EW-LS}_{t_0}(\mathbb{W}, \widehat{\kappa}) : \qquad & \sup_{\mathcal{P}_0 \in \mathcal{A}} \Bigg\{ E_{\mathcal{P}_0}^{\mathcal{X}_0^-, t_0^-} \Bigg[\sum_{i=0}^{M} q_i \;+\; \hat{\kappa} \; \min(W_T - \mathbb{W}, 0) + \epsilon W_T \\
& \qquad \Bigg| \mathcal{X}(t_0^-) = (s,b) \Bigg] \Bigg\} , \qquad (4.19) \\
\text{subject to} \qquad & \Big\{ \text{Conditions (4.5)} \qquad .
\end{aligned}
$$

Note that we notationally distinguish risk aversion parameters for EW-ES and EW-LS to describe their precise connection. We summarize the relationship between EW-ES and EW-LS in Proposition 4.1 (see also Forsyth (2020a)).

Proposition 4.1 (Optimal EW-ES strategy solves EW-LS)**.**

(i) The pre-commitment strategy $\mathcal{P}^*$ which solves EW-ES$_{t_0}(\alpha,\kappa)$ (4.7) *is a solution to EW-LS$_{t_0}(\mathbb{W},\frac{\kappa}{\alpha})$* (4.19) *with the fixed wealth level $\mathbb{W} = \mathbb{W}^*$ defined in* (4.17)*.*

(ii) Conversely, an optimal control for EW-LS$_{t_0}(\mathbb{W},\frac{\kappa}{\alpha})$ (4.19) *with the fixed wealth level $\mathbb{W} = \mathbb{W}^*$ given by* (4.17)*, solves EW-ES$_{t_0}(\alpha,\kappa)$* (4.7)*.*

Proof.

(i) Let $\mathcal{P}_0^*$ solve (4.7). Then it solves (4.8) due to equivalence between (4.8) and (4.7). Consequently $\mathcal{P}_0^*$ also solves the linear shortfall problem EW-LS$_{t_0}(\mathbb{W}^*,\frac{\kappa}{\alpha})$ in (4.19), i.e., $\mathcal{P}_0^*$ solves

$$
\begin{aligned}
\text{EW-LS}_{t_0}(\mathbb{W}, \hat{\kappa}) : \qquad & \sup_{\mathcal{P}_0 \in \mathcal{A}} \Bigg\{ E_{\mathcal{P}_0}^{\mathcal{X}_0^-, t_0^-} \Bigg[\sum_{i=0}^{M} q_i \;+\; \hat{\kappa} \min(W_T - \mathbb{W}, 0) \\
& \qquad + \epsilon W_T \Bigg| (s,b) \Bigg] \Bigg\} \\
\text{subject to} \; & \Big\{ \text{Conditions (4.5)} \qquad ,
\end{aligned}
$$

with $\hat{\kappa} = \frac{\kappa}{\alpha}$, $\mathbb{W} = \mathbb{W}^*$, and $\mathbb{W}^*$ defined in (4.17).

(ii) Assume that $\mathcal{P}_0^*$ solves EW-LS$_{t_0}(\mathbb{W}^*, \hat{\kappa})$, (4.19), with $\hat{\kappa} = \frac{\kappa}{\alpha}$ and $\mathbb{W}^*$ defined in (4.17). Then $\mathcal{P}_0^*$ solves

$$\begin{aligned} \sup_{\mathcal{P}_0 \in \mathcal{A}} \Bigg\{ E_{\mathcal{P}_0}^{\mathcal{X}_0^-, t_0^-} \Bigg[& \sum_{i=0}^{M} q_i \ + \ \kappa(\mathbb{W}^* + \frac{1}{\alpha} \min(W_T - \mathbb{W}^*, 0) \\ & + \epsilon W_T \Bigg| (s,b) \Bigg] \Bigg\} \\ \text{subject to } & \Big\{ \text{Conditions (4.5)} \quad , \end{aligned}$$

Applying $\mathbb{W}^*$ defined in (4.17), then $\mathcal{P}_0^*$ solves (4.8), and hence (4.7).

□

Let

$$\begin{aligned} \mathcal{D}_{ES} &= \{(\alpha, \kappa) \mid 0 < \alpha < 1 \ ; \ \kappa > 0\} \\ \mathcal{D}_{LS} &= \{(\mathbb{W}, \kappa) \mid \mathbb{W} \in \mathbb{R} \ ; \ \kappa > 0\} \ . \end{aligned} \tag{4.20}$$

Define

$$\begin{aligned} \mathcal{H}_{\text{ES}}^* &= \{\mathcal{P}_0^* : \ \mathcal{P}_0^* \text{ solves EW-ES}_{t_0}(\alpha, \kappa)(4.7) \text{ for some } (\alpha,\kappa) \in \mathcal{D}_{ES}\} \\ \mathcal{H}_{\text{LS}}^* &= \{\mathcal{P}_0^* : \ \mathcal{P}_0^* \text{ solves EW-LS}_{t_0}(\mathbb{W}, \hat{\kappa})(4.19) \text{ for some } (\mathbb{W},\hat{\kappa}) \in \mathcal{D}_{LS}\} \ . \end{aligned} \tag{4.21}$$

We then have the following Corollary, which follows from Proposition 4.1:

Corollary 4.1. *Let $\mathcal{H}_{ES}^*$ and $\mathcal{H}_{LS}^*$ be defined in* (4.21)*. Then the set $\mathcal{H}_{ES}^*$ of optimal controls for Problem EW-ES$_{t_0}$ is a subset of the set $\mathcal{H}_{LS}^*$ of optimal controls for Problem EW-LS$_{t_0}$.*

4.4 Time inconsistent EW-ES and time consistent EW-LS

While Proposition 4.1 indicates that EW-ES$_{t_0}$ and EW-LS$_{t_0}$ share a common solution when the wealth level $\mathbb{W} = \mathbb{W}^*$, these two dynamic optimization formulations have different properties in terms of time consistency. To see this, we first recall the concept of time consistency and relate its relevance to the EW-ES$_{t_0}(\alpha,\kappa)$ problem, (4.8).

Consider the optimal control $\mathcal{P}_0^* = (\mathcal{P}^*)^{t_0}$ computed at t_0 from problem (4.8) at all rebalancing times,

$$(\mathcal{P}^*)^{t_0}(\mathcal{X}(t_i^-), t_i) \ , \ i = 0, \ldots, M \ , \tag{4.22}$$

i.e., (4.22) denotes the optimal control $(\mathcal{P}^*)^{t_0}$ at any time $t_i \geq t_0$, as a function of the state variables $\mathcal{X}(t)$.

Next we solve the problem (4.8) starting at a later time $t_k, k > 0$ and denote the optimal control starting at t_k is denoted by:

$$(\mathcal{P}^*)^{t_k}(\mathcal{X}(t_i^-), t_i) \ , \ i = k, \ldots, M \ . \tag{4.23}$$

In general, the solution of (4.8) computed at t_k is not equivalent to the solution computed at t_0:

$$(\mathcal{P}^*)^{t_k}(\mathcal{X}(t_i^-), t_i) \neq (\mathcal{P}^*)^{t_0}(\mathcal{X}(t_i^-), t_i) \ ; \ i \geq k > 0. \tag{4.24}$$

This non-equivalence makes problem (4.8) *time inconsistent*, implying that the optimal control computed at t_k, $k > 0$, deviates from the control determined at time t_0. The optimal control

$\mathcal{P}_0^* = (\mathcal{P}^*)^{t_0}$ determined at the initial time is considered a *pre-commitment* control since the investor would need to commit to following the strategy at all times following t_0, even if the optimal control recomputed at future time becomes different. Some authors describe pre-commitment controls as non-implementable because of the incentive to deviate from the initial control.

Following Proposition 4.1, the pre-commitment control for EW-ES$_{t_0}$ (4.8), fortunately, can be shown to be optimal for EW-LS$_{t_0}(\mathbb{W},\hat{\kappa})$, for which $\mathbb{W}$ is fixed at the optimal value (at time zero) in (4.17).

With a fixed $\mathbb{W}$, EW-LS$_{t_0}(\mathbb{W},\kappa/\alpha)$ uses a target-based linear shortfall as its measure of risk, and EW-LS$_{t_0}$ is trivially time consistent. Furthermore, $\mathbb{W}$ has the convenient interpretation of a disaster level of final wealth, as specified at time zero.

While the pre-commitment strategy $\mathcal{P}^*$ from EW-ES$_{t_0}(\alpha,\kappa)$, (4.8), is time inconsistent when viewed as a solution to EW-ES, this strategy is time consistent with respect to EW-LS$_{t_0}(\mathbb{W}^*,\frac{\kappa}{\alpha})$ with the fixed wealth level $\mathbb{W}^*$. In other words, conditional on information at t_n and fixed $\mathbb{W}^*$, the future decision $\{(\mathcal{P}^*)^{t_n}(\mathcal{X}(t_i^-),t_i)\ ;\ i = n,\ldots,M\}$ of the optimal pre-commitment EW-ES control, computed at t_0, solves

$$\begin{aligned} \text{EW-LS}_{t_n}(\mathbb{W}^*,\kappa/\alpha): \qquad & \sup_{\mathcal{P}_n\in\mathcal{A}} \Bigg\{ E_{\mathcal{P}_n}^{\mathcal{X}_n^-,t_n^-}\Bigg[\ \sum_{i=n}^{M} q_i\ +\ \frac{\kappa}{\alpha}\min(W_T-\mathbb{W}^*,0) \qquad (4.25) \\ & \qquad +\epsilon W_T \Bigg| \mathcal{X}(t_n^-) = (s,b) \Bigg]\Bigg\}, \end{aligned}$$

for any given permissible stock and bond value pair (s,b).

Remark 4.2 (EW-ES $\rightarrow$ EW-LS). *Proposition 4.1 essentially tells us that any optimal control $\mathcal{P}^*$ from EW-ES problem (4.8), solves some EW-LS problem (4.25) with a fixed wealth level $\mathbb{W}^*$. Since EW-LS is time consistent, the EW-ES optimal control $\mathcal{P}^*$ is time consistent when Pareto optimality is assessed with EW-LS with this fixed wealth level $\mathbb{W}^*$.*

Since the optimal control $\mathcal{P}^*$ for EW-ES$_{t_0}(\alpha,\kappa)$ solves EW-LS$_{t_n}(\mathbb{W}^*,\kappa/\alpha)$ at any t_n, where $\mathbb{W}^*$ is the α-VaR of the conditional terminal wealth W_T^*, conditional on $W_0^* = s+b$, we can regard $\mathcal{P}^*$ as an induced time consistent strategy for EW-LS$_{t_n}(\mathbb{W}^*,\kappa/\alpha)$ (Strub et al., 2019). Consequently the investor has no incentive to deviate from the induced time consistent strategy, determined at time zero. Hence this policy is implementable.

For more detailed analysis concerning the subtle distinctions involved in pre-commitment, time consistent, and induced time consistent strategies, please consult Bjork and Murgoci (2010; 2014); Vigna (2014; 2017); Strub et al. (2019); Forsyth (2020a); Bjork et al. (2021).

4.5 Further relationship between EW-ES and EW-LS problem

Problem EW-ES$_{t_0}(\alpha,\kappa)$ requires specification of the parameter pair (α,κ) while problem EW-LS$_{t_0}(\mathbb{W},\hat{\kappa})$ needs stipulation of parameter pair $(\mathbb{W},\hat{\kappa})$. From Proposition 4.1 (ii), we learn that, given a value of $\mathbb{W}$ from equation (4.17) we can solve problem Problem EW-LS$_{t_0}(\mathbb{W},\hat{\kappa})$, which generates a control which is an optimal control for problem EW-ES$_{t_0}(\alpha,\alpha\hat{\kappa})$.

However, given an arbitrary value of $\mathbb{W}$, for which a solution to Problem EW-LS$_{t_0}(\mathbb{W},\hat{\kappa})$ exists, what is the relation of the optimal control for this problem to the optimal control for Problem EW-ES$_{t_0}(\alpha,\kappa)$?

To connect an optimal EW-LS solution $\mathcal{P}_0^*$ to EW-ES$_{t_0}$, we define

$$\alpha_{\hat{\kappa}}^*(\mathbb{W}) = \text{prob}(W_T^* < \mathbb{W}), \quad W_{T^*} \text{ is the terminal wealth of } \mathcal{P}_0^* \text{ which solves EW-LS}_{t_0}(\mathbb{W},\hat{\kappa}) \qquad (4.26)$$

Remark 4.3 (Construction of $\alpha^*_{\hat{\kappa}}(\mathbb{W})$)**.** *Given* $(\mathbb{W}, \hat{\kappa})$*, and an optimal control* $\mathcal{P}_0^*(\mathbb{W}, \hat{\kappa})$ *which solves Problem EW-LS*$_{t_0}(\mathbb{W}, \hat{\kappa})$*, then we can determine* $\alpha^*_{\hat{\kappa}}(\mathbb{W})$ *from*

$$\alpha^*_{\hat{\kappa}}(\mathbb{W}) \quad = \quad E_{\mathcal{P}_0^*(\mathbb{W},\hat{\kappa})}[\mathbf{1}_{\{W_T{*}<\mathbb{W}\}}] \ . \tag{4.27}$$

To ensure a proper correspondence to EW-ES$_{t_0}$, we consider solution to EW-LS$_{t_0}$ with $0 < \alpha^*_{\hat{\kappa}}(\mathbb{W}) < 1$, i.e., we consider a restricted domain for EW-LS$_{t_0}$ as:

$$\mathcal{D}^+_{LS} \quad = \quad \{(\mathbb{W}, \hat{\kappa}) \mid \ 0 < \alpha^*_{\hat{\kappa}}(\mathbb{W}) < 1 \ \text{ and } \hat{\kappa} > 0\} \ . \tag{4.28}$$

Assumption 4.1 (invertibility of $\alpha^*_{\hat{\kappa}}(\mathbb{W})$)**.** *The function* $\alpha^*_{\hat{\kappa}}(\mathbb{W})$ *in* (4.26) *is well defined and is invertible at* $(\mathbb{W},\hat{\kappa}) \in \mathcal{D}^+_{LS}$*, i.e., for any* $\mathbb{W}' \neq \mathbb{W}, (\mathbb{W}', \hat{\kappa}) \in \mathcal{D}^+_{LS}, \alpha^*_{\hat{\kappa}}(\mathbb{W}') \neq \alpha^*_{\hat{\kappa}}(\mathbb{W})$*.*

Note that here we only assume that, for each given $\mathbb{W}$ and $\hat{\kappa}$, EW-LS$_{t_0}(\mathbb{W}, \hat{\kappa})$ yields a unique probability value $\alpha^*_{\hat{\kappa}}(\mathbb{W})$ but we do not assume uniqueness of the optimal controls for EW-LS$_{t_0}(\mathbb{W}, \hat{\kappa})$.

Proposition 4.2 below establishes an equivalence of EW-ES$_{t_0}$ and EW-LS$_{t_0}$, under the assumption that the function $\alpha^*_{\hat{\kappa}}(\mathbb{W})$ is well defined and invertible.

Proposition 4.2 (Relationship between EW-LS$_{t_0}$ and EW-LS$_{t_0}$ for general $\mathbb{W}$)**.** *Suppose Assumption 4.1 holds at* $(\mathbb{W}, \hat{\kappa}) \in \mathcal{D}^+_{LS}$*, then a solution to EW-LS*$_{t_0}(\mathbb{W}, \hat{\kappa})$ *is a solution to EW-ES*$_{t_0}(\alpha^*_{\hat{\kappa}}(\mathbb{W}), \alpha^*_{\hat{\kappa}}(\mathbb{W})\hat{\kappa})$*, with* $(\alpha^*_{\hat{\kappa}}(\mathbb{W}), \alpha^*_{\hat{\kappa}}(\mathbb{W})\hat{\kappa}) \in \mathcal{D}_{ES}$*.*

Proof. Consider EW-LS$_{t_0}(\mathbb{W}, \hat{\kappa})$ for a given $(\mathbb{W},\hat{\kappa}) \in \mathcal{D}^+_{LS}$. Let $\alpha^*_{\hat{\kappa}}(\mathbb{W})$ be defined in (4.26). Consider EW-ES$_{t_0}(\alpha^*,\alpha^*\hat{\kappa})$ where $\alpha^* = \alpha^*_{\hat{\kappa}}(\mathbb{W})$. Note that by definition of $\mathcal{D}^+_{LS}$, we must have $(\alpha^*,\alpha^*\hat{\kappa}) \in \mathcal{D}_{ES}$. Proposition 4.1 (i) shows that a solution of EW-ES$_{t_0}(\alpha^*,\hat{\kappa}\alpha^*)$ is a solution to linear shortfall EW-LS$_{t_0}(\mathbb{W}^*,\hat{\kappa})$ problem for $\mathbb{W}^*$ defined in (4.17) with prob$(W^*_T < \mathbb{W}^*) = \alpha^*_{\hat{\kappa}}(\mathbb{W}^*) = \alpha^*$. Hence

$$\alpha^*_{\hat{\kappa}}(\mathbb{W}) = \alpha^*_{\hat{\kappa}}(\mathbb{W}^*) = \alpha^*.$$

Since $\alpha^*_{\hat{\kappa}}(\mathbb{W})$ is invertible, we have that $\mathbb{W} = \mathbb{W}^*$. Applying Proposition 4.1 (ii), using $\mathbb{W} = \mathbb{W}^*$ given in (4.17), a solution to EW-LS$_{t_0}(\mathbb{W},\hat{\kappa})$ solves EW-ES$_{t_0}(\alpha^*,\alpha^*\hat{\kappa})$, where $\alpha^* = \alpha^*_{\hat{\kappa}}(\mathbb{W})$. This completes the proof. □

Applying Corollary 4.1 and Proposition 4.2, we obtain the following Corollary 4.2.

Corollary 4.2. *Suppose Assumption 4.1 holds for any* $(\mathbb{W},\hat{\kappa}) \in \mathcal{D}^+_{LS}$*. Let* $\mathcal{H}^*_{ES}$ *and* $\mathcal{H}^*_{LS}$ *be defined in* (4.21)*. Then the set* $\mathcal{H}^*_{ES}$ *of optimal controls for Problem EW-ES*$_{t_0}$ *is identical to the set* $\mathcal{H}^{*+}_{LS}$ *of optimal controls for Problem EW-LS*$_{t_0}$*, where*

$$\mathcal{H}^{*+}_{LS} = \{\mathcal{P}_0^*(\mathbb{W},\hat{\kappa}) \in \mathcal{H}^*_{LS} \text{ and } (\mathbb{W},\hat{\kappa}) \in \mathcal{D}^+_{LS}\}.$$

Proof. From Proposition 4.1, any optimal solution $\mathcal{P}_0^*$ of EW-ES$_{t_0}$ satisfies $0 < \alpha^*_{\hat{\kappa}}(\mathbb{W}^*) < 1$, $\mathbb{W}^*$ defined in (4.17). Hence we have

$$\mathcal{H}^*_{\text{ES}} \subset \mathcal{H}^{*+}_{\text{LS}}.$$

Conversely, following Proposition 4.2, if $\mathcal{P}_0^* \in \mathcal{H}^{*+}_{\text{LS}}$, then $\mathcal{P}_0^* \in \mathcal{H}^*_{\text{ES}}$, i.e., $\mathcal{P}_0^* \in \mathcal{H}^*_{\text{ES}}$. Hence

$$\mathcal{H}^*_{\text{ES}} \equiv \mathcal{H}^{*+}_{\text{LS}}.$$

□

Corollary 4.2 essentially states that, under Assumption 4.1, the set of optimal controls associated with all EW-ES$_{t_0}$ Pareto efficient frontier curves, $(\alpha, \kappa) \in \mathcal{D}_{ES}$ is identical to the set of optimal controls for all EW-LS$_{t_0}$ Pareto efficient frontier curves with $(\mathbb{W}, \hat{\kappa}) \in \mathcal{D}^+_{LS}$.

Remark 4.4 (Significance of Propositions 4.1 and 4.17)**.** *Proposition 4.1 (i) shows that any control which solves Problem EW-ES*$_{t_0}$ *solves the Problem EW-LS*$_{t_0}$ *with fixed* $\mathbb{W}$ *given by equation (4.17). Proposition 4.1 (ii) informs us that for certain values of* $(\mathbb{W}, \hat{\kappa})$*, the optimal control for Problem EW-LS*$_{t_0}$ *also solves problem EW-ES*$_{t_0}$*. This is also true more generally, for points* $(\mathbb{W},\hat{\kappa})$ *satisfying Assumption 4.1. It would be interesting to discover conditions on Problem EW-LS*$_{t_0}$ *which are required to guarantee that Assumption 4.1 holds. We leave this for future work.*

Remark 4.5 (Numerical experiments: EW-LS$_{t_0}$ $\rightarrow$ EW-ES$_{t_0}$)**.** *Problems EW-LS*$_{t_0}$ *and EW-ES*$_{t_0}$ *are solved numerically, as discussed in Appendix B. Equation (4.27) is approximated using Monte Carlo methods. For values of* $(\hat{\kappa}, \mathbb{W})$ *such that* $\alpha^*_{\hat{\kappa}}(\mathbb{W})$ *is small (i.e.* $\alpha^*_{\hat{\kappa}} < .02$*), Proposition 4.2 does not appear to hold. This may be a result of numerical errors in approximating the* α*-VAR for small* α*.*

5 Numerical Comparison of Different Risk-Reward Pairs

5.1 Data

We use data from the Center for Research in Security Prices (CRSP) on a monthly basis over the 1926:1-2023:12 period.[10] Our base case tests use the CRSP US 30 day T-bill for the bond asset and the CRSP value-weighted total return index for the stock asset. This latter index includes all distributions for all domestic stocks trading on major U.S. exchanges. All of these various indexes are in nominal terms, so we adjust them for inflation by using the U.S. CPI index, also supplied by CRSP. We use real indexes since investors funding retirement spending should be focused on real (not nominal) wealth goals.

We use the parametric model for the real stock index and real constant maturity bond index described in Appendix A.

Remark 5.1 (Choice of 30-day T-bill for the bond index)**.** *It might be argued that the bond index should hold longer-dated bonds such as 10-year Treasuries since this would allow the investor to harvest the term premium. Long-term bonds enjoyed high real returns during 1990-2022. However, it is unlikely that this will continue to be true over the next 30 years. For example, during the period 1950-1983, long term bonds had negative real returns (Hatch and White, 1985), while short-term T-bills had positive real returns. If one imagines that the next 30 years will be a period with inflationary pressures, this suggests that the defensive asset should be short-term T-bills. Note that the historical real return of short-term T-bills over 1926:1-2023:12 is approximately zero. Hence our use of T-bills as the defensive asset is a conservative approach going forward.*

Remark 5.2 (Sensitivity to Calibrated Parameters)**.** *Some readers might suggest that the stochastic processes (A.3-A.4) are simplistic, and perhaps inappropriate. However, we will test the optimal strategies (computed assuming processes (A.3-A.4)) with calibrated parameters in Table A.1 using bootstrap resampled historical data (see Section 5.2 below). The computed strategy seems surprisingly robust to model misspecification. Similar results have been noted for the case of multi-period mean-variance controls (van Staden et al., 2021). We conjecture that this robustness is due to the self-correcting nature of feedback controls.*

[10]More specifically, results presented here were calculated based on data from Historical Indexes, ©2024 Center for Research in Security Prices (CRSP), The University of Chicago Booth School of Business. Wharton Research Data Services (WRDS) was used in preparing this article. This service and the data available thereon constitute valuable intellectual property and trade secrets of WRDS and/or its third-party suppliers.

Data series	Optimal expected block size $\hat{b}$ (months)
Real 30-day T-bill index	50.805
Real CRSP value-weighted index	3.17535

TABLE 5.1: *Optimal expected blocksize $\hat{b} = 1/v$ when the blocksize follows a geometric distribution $Pr(b = k) = (1 - v)^{k-1}v$. The algorithm in Patton et al. (2009) is used to determine $\hat{b}$. Historical data range 1926:1-2023:12.*

5.2 Historical Market

We compute and store the optimal controls based on the parametric model (A.3-A.4) as for the synthetic market case. However, we compute statistical quantities using the stored controls, but using bootstrapped historical return data directly. In this case, we make no assumptions concerning the stochastic processes followed by the stock and bond indices. We remind the reader that all returns are inflation-adjusted. We use the stationary block bootstrap method (Politis and Romano, 1994; Politis and White, 2004; Patton et al., 2009; Cogneau and Zakalmouline, 2013; Dichtl et al., 2016; Cavaglia et al., 2022; Simonian and Martirosyan, 2022; Anarkulova et al., 2022).

A key parameter is the expected blocksize. Sampling the data in blocks accounts for serial correlation in the data series. We use the algorithm in Patton et al. (2009) to determine the optimal blocksize for the bond and stock returns separately, see Table 5.1. We use a paired sampling approach to simultaneously draw returns from both time series. In this case, a reasonable estimate for the blocksize for the paired resampling algorithm would be about 2.0 years. We will give results for a range of blocksizes as a check on the robustness of the bootstrap results. Detailed pseudo-code for block bootstrap resampling is given in Forsyth and Vetzal (2019).

5.3 Investment Scenario

Table 5.2 shows our base case investment scenario. We use thousands of dollars as our units of wealth. For example, a withdrawal of 40 per year corresponds to \$40,000 per year (all values are real, i.e. inflation-adjusted), with an initial wealth of 1000 (i.e. \$1,000,000). This would correspond to the use of the four per cent rule (Bengen, 1994). Recall that we assume that the investor has real estate, which is in a separate mental bucket (Shefrin and Thaler, 1988). Real estate is a hedge of last resort, used to fund required minimum cash flows (Pfeiffer et al., 2013). We assume that the retiree owns mortgage free real estate worth \$400,000, of which \$200,000 can be easily accessed using a reverse mortgage.

5.4 Numerical Results

We use the numerical method described in (Forsyth, 2022; Forsyth et al., 2024) to compute the optimal controls, which is based on solving a Partial Integro-Differential Equation (PIDE), combined with discretizing the controls and finding the optimal values by exhaustive search. A brief overview is given in Appendix B.

We compute optimal strategies from EW-ES$_{t_0}(\alpha, \kappa)$ with $\alpha = 0.05$ and $\kappa > 0$. For EW-LS$_{t_0}(\mathbb{W},\hat{\kappa})$ and EW-PS$_{t_0}(\mathbb{W},\hat{\kappa})$, we compute optimal strategies with $\mathbb{W} = 0$ and $\hat{\kappa} > 0$.

Investment horizon T (years)	30.0
Equity market index	CRSP Cap-weighted index (real)
Bond index	30-day T-bill (US) (real)
Initial portfolio value W_0	1000
Mortgage free real estate	400
Cash withdrawal/rebalancing times	$t = 0,1.0, 2.0, \ldots, 29.0$
Maximum withdrawal (per year)	$q_{\max} = 60$
Minimum withdrawal (per year)	$q_{\min} = 30$
Equity fraction range	[0,1]
Borrowing spread μ_c^b	0.03
Rebalancing interval (years)	1.0
Target Wealth $\mathbb{W}$ (EW-xS, $x = \{P,L\}$)	0.0
α (EW-ES)	.05
Stabilization ϵ (see equation (4.4))	-10^{-4}
Market parameters	See Table A.1

TABLE 5.2: *Input data for examples. Monetary units: thousands of dollars.*

5.5 Convergence

Appendix B.1 shows convergence as the number of grid nodes increases, for a single point on the synthetic market EW-LS efficient frontier. It is perhaps more instructive to examine the convergence of the efficient frontiers. Figure 5.1 shows the convergence of the EW-LS frontier, as a function of the PIDE nodes. The curves for different numbers of nodes essentially overlap, indicating satisfactory convergence. Similar results were obtained for the other strategies.

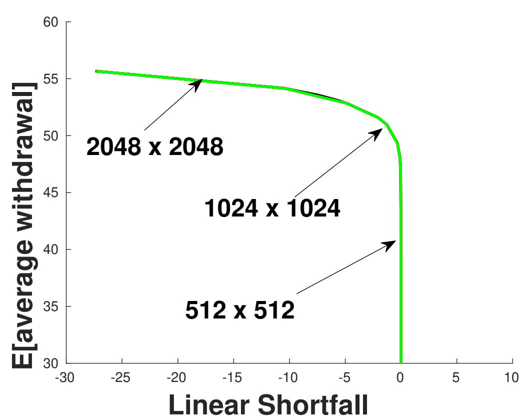

FIGURE 5.1: *EW-LS convergence test. Real stock index: deflated real capitalization weighted CRSP, real bond index: deflated 30 day T-bills. Scenario in Table 5.2. Parameters in Table A.1. The optimal control is determined by solving the PIDEs as described in Appendix B. Grid refers to the grid used in the algorithm in Appendix B: $n_x \times n_b$, where n_x is the number of nodes in the $\log s$ direction, and n_b is the number of nodes in the $\log b$ direction. Units: thousands of dollars (real). The controls are stored, and then the final results are obtained using a Monte Carlo method, with 2.56×10^6 simulations. Target wealth $\mathbb{W} = 0.0$.*

5.6 Stabilization term

In Appendix C, we show the effect of changing the sign of the stabilization term for the EW-PS problem on the CDF of the final wealth W_T. The stabilization term has almost no effect on the CDF near $\mathbb{W} = 0$, but does change the CDF for large values of wealth. This is because the choice of controls for large values of wealth, as $t \to T$ is essentially arbitrary. For large values of realized wealth, the investor can choose 100% bonds or 100% stocks, and the objective function will be almost unaffected.[11]

5.7 Efficient Frontiers: EW-LS, EW-PS, EW-ES

In this section, we compare efficient frontier curves computed from EW-ES$_{t_0}(\alpha,\kappa)$ with fixed $\alpha = 0.05$ and $\kappa > 0$, and EW-xS$_{t_0}(\mathbb{W},\hat{\kappa})$ (x =P,L) with $\mathbb{W} = 0$ and $\hat{\kappa} > 0$. We choose this comparison setting since it seems more immediately relevant from a retiree's perspective.

We assess the performance of these strategies in the performance domain (EW,LS), (EW,PS), and (EW,ES) in Figures 5.2, 5.3(a), and 5.3(b) respectively.

Since all three formulations share the same reward, the top left sides of efficient frontiers from all strategies are expected to converge asymptotically (as risk aversion parameter goes to zero) in all performance domains (EW,LS), (EW,PS), and (EW,ES).

Note that efficient frontier curves in either performance domain (EW,ES) or (EW,LS), from EW-ES$_{t_0}(\alpha,\kappa)$ and EW-LS$_{t_0}(\mathbb{W},\hat{\kappa})$, for fixed α and $\mathbb{W}$, are not expected to coincide, except possibly at single points.

As the risk aversion parameter increases, efficient frontiers on the right side from different formulations are expected to deviate from each other more significantly. Overall, 5.2, Figure 5.3(a), and 5.3(b) do demonstrate larger differences in efficient frontier curves on the right side, see particularly EW-ES frontiers in Figure 5.3(b). This confirms that the choice of objective function is important in achieving risk control. Subsequently we compare and contrast efficient frontiers in more detail.

5.7.1 EW-LS

Figure 5.2 plots frontier curves in the (EW,LS) domain. We compute EW-LS, EW-ES and EW-PS optimal controls, but plot their (EW,LS) performance measures in the same figure. Naturally the frontier curve of the EW-LS control must plot above all the other curves (since the objective function of EW-LS aligns with the specified measures). However, it is interesting to see that the EW-ES and EW-PS controls are not overly suboptimal, relative to EW-LS$_{t_0}(\mathbb{W} = 05,\hat{\kappa})$, using (EW,LS) criteria.

From Proposition 4.1, we expect that there is a point (with target wealth $\mathbb{W} = 0$) at which the EW-ES and EW-LS curve coincide. In Figure 5.2, we can see that this point occurs at $EW \simeq 52.3$. Figure 5.2 also shows the results for the Bengen strategy (Bengen, 1994).[12] We can see that the Bengen strategy is considerably suboptimal compared to any of the other strategies. However, it is only fair to point out that the Bengen strategy always withdraws 40 per year (units thousands), while the other strategies have minimum withdrawals of 30 per year.

[11] The 94 year old Warren Buffet, whose net worth exceeds 145 billion USD, can choose to invest either 100% in stocks or 100% in bonds, and will never run out of savings.

[12] Recall that the recommended policy is to withdraw 4% of the initial capital per year, inflation adjusted, and to rebalance to a weight of 50% stocks annually. The 4% withdrawal would correspond to 40 per year for our example.

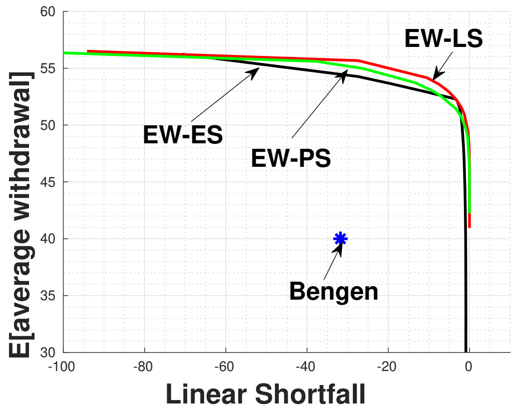

FIGURE 5.2: *EW-LS efficient frontier. Real stock index: deflated real capitalization weighted CRSP, real bond index: deflated 30 day T-bills. Scenario in Table 5.2. Parameters in Table A.1. Synthetic market. Controls computed using EW-PS and EW-ES, and results plotted in terms of EW-LS criteria. The EW-LS frontier plots above the the controls computed using EW-PS and EW-ES objective functions. The Bengen control withdraws 40 per year, and rebalances annually to 50% bonds and 50% stocks. The wealth target level* $\mathbb{W} = 0$ *for both* EW-LS$_{t_0}$ *and* EW-PS$_{t_0}$.

5.7.2 EW-PS

Figure 5.3(a) plots the EW-PS efficient frontier. Along the x-axis we plot $Prob[W_T > 0] = 1 - Prob[W_T < 0]$, to produce consistent shapes for the frontiers. As before, we compute the EW-ES and EW-LS efficient controls, but plot them using PS as a risk measure. As expected, the EW-PS frontier plots above the other curves (it is, after all, the efficient strategy according to the $Prob[W_T > 0]$ risk measure).

There is somewhat more variation in these curves compared to Figure 5.2. In particular, the EW-PS and EW-LS curves generate $Prob[W_T > 0] \simeq 0.9998$ for the largest values of κ (the right hand most point on the curves). In contrast, the EW-LS strategy never gets above $Prob[W_T > 0] \simeq 0.994$. We also see that the EW-LS curve flat-tops to the left of $EW \simeq 52$.[13]

5.7.3 EW-ES

Figure 5.3(b) shows the EW-ES efficient frontier. We also show (EW,ES) measures for optimal EW-PS$_{t_0}(0,\kappa)$ and EW-LS$_{t_0}(0,\kappa)$ strategies. The curves for EW-PS and EW-LS are very similar. However, for $ES > 0$, the EW-ES curve is dramatically different. This can be explained as follows.

The EW-ES strategy moves towards maximizing ES as κ becomes large. This comes at the expense of decreased $Prob[W_t > 0]$ (from Figure 5.3(a)). On the other hand, the EW-LS and EW-PS strategies have no risk if $W_T > 0$, so focus entirely on increasing EW, if $W_t > 0$ as $t \rightarrow T$. Effectively, this means that for the EW-LS and EW-PS strategies, it does not make sense to consider points in the efficient frontier which are below the *knee* of the curves. To the left of the *knee* of the curves, EW-LS is very close to the EW-ES curve.

Recall that we have assumed that the retiree can access \$200K using a reverse mortgage with real estate as collateral. Consequently, as a rule of thumb, any point on any frontier which has $ES > -200$ is acceptable from a risk management point of view. In other words the mean of the

[13]If we extend the x-axis to the left, then, eventually, all three curves meet. However, these points have an uncomfortably large $Prob[W_T] < 0$, hence are not of practical interest.

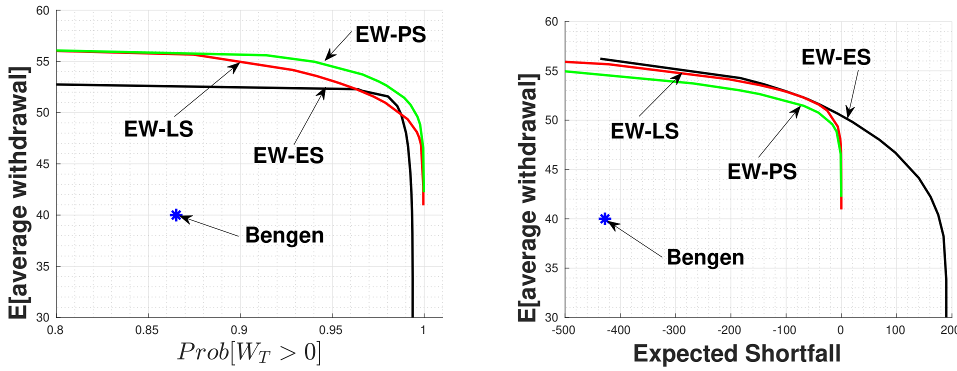

(a) *EW-PS efficient frontier. Results for EW-LS and EW-ES also shown.*

(b) *EW-ES efficient frontier. Results for EW-LS and EW-PS also shown.*

FIGURE 5.3: *EW-PS and EW-ES efficient frontiers. Real stock index: deflated real capitalization weighted CRSP, real bond index: deflated 30 day T-bills. Scenario in Table 5.2. Parameters in Table A.1. Synthetic market. The Bengen control withdraws 40 per year, and rebalances annually to 50% bonds and 50% stocks. Target wealth $\mathbb{W} = 0$ for EW-LS and EW-PS.*

worst 5% of the outcomes can be hedged using real estate. In particular, we can see that the Bengen strategy fails this risk management test.

5.7.4 Summary of efficient frontier comparison

It is relevant to compare performance of optimal strategies using risk measures which are not directly included in their respective objective functions. This helps an investor understand consequences of implementing a specific strategy from in terms of different but relevant performance measures.

Our first observation is that in all cases, whatever the strategy or risk measure, the Bengen strategy is significantly sub-optimal. We also make the following additional observations:

- Firstly recall that we use the same target wealth level $\mathbb{W} = 0$ for both EW-LS$_{t_0}$ and EW-PS$_{t_0}$. We observe that their frontier curves are close in all three measurement domains, (EW,LS), (EW,PS) and (EW,ES), even asymptotically as the risk aversion parameter $\kappa \to +\infty$. This suggests that choosing EW-LS$_{t_0}$ also leads to good performance in terms of EW-PS$_{t_0}$. Furthermore, since linear shortfall is an expectation of piecewise linear shortfall, i.e., $E(\max(W_T - \mathbb{W}, 0))$, while the probability function is the expectation of a discontinuous indicator function, i.e., $E(\mathbf{1}_{W_T < \mathbb{W}})$, consequently solving EW-LS$_{t_0}$ can be computationally preferable to solving EW-PS$_{t_0}$.

- Choosing a suitable risk measure as part of the objective function which aligns with the desired decumulation goals does matter. Different risk measures can lead to very different performing strategies. This is particularly important in decumulation. For example, Figure 5.3(a) shows that the optimal EW-ES$_{t_0}$ strategy is inefficient at minimizing the probability of negative terminal wealth. The smallest probability of negative wealth achieved is at the expense of steeply diminishing reward. Similarly Figure 5.3(b) shows that, with the wealth target $\mathbb{W} = 0$, the 5% ES risk associated with the optimal EW-LS$_{t_0}$ and EW-PS$_{t_0}$ strategies as the risk aversion parameter $\hat{\kappa} \to +\infty$ is far from the optimal 5%-ES risk achievable.

- While Figure 5.2 seems to indicate that all the strategies perform reasonably well in terms of the LS risk measure, we note that there is a similar steeper drop from the optimal EW-ES$_{t_0}$

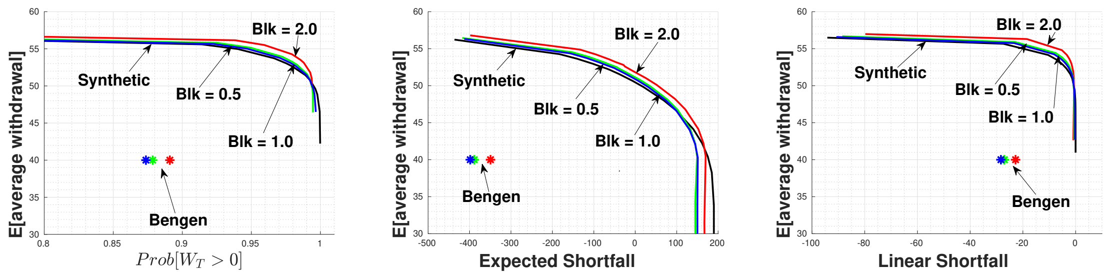

(a) *EW-PS efficient frontier, bootstrapped simulations.*

(b) *EW-ES efficient frontier, bootstrapped simulations.*

(c) *EW-LS efficient frontier, bootstrapped simulations.*

FIGURE 5.4: *Optimal controls computed using the synthetic market model. These controls tested using bootstrapped historical data. Expected blocksizes (years) shown.* 10^6 *bootstrap resamples. Real stock index: deflated real capitalization weighted CRSP, real bond index: deflated 30 day T-bills. Scenario in Table 5.2. Parameters in Table A.1. The Bengen control withdraws 40 per year, and rebalances annually to 50% bonds and 50% stocks. The Bengen results are also shown for expected blocksizes of* $0.5, 1.0, 2.0$ *years.*

strategy as the risk aversion parameter goes to $+\infty$. We further note that the scales of the horizontal axis in Figure 5.2 and Figure 5.3(a) are very different. Optimal EW-ES$_{t_0}$ strategies are unable to achieve the minimum LS risk and the smallest LS risk strategy is achieved at the expense of suboptimal rewards.

From Figure 5.3(a) we can see that, in terms of the PS risk measure, EW-LS plots a bit below the optimal EW-PS frontier. However, the EW-ES curve has a very unusual behaviour (in terms of PS risk). Any increase in EW above about 53 causes a large decrease in $Prob[W_T > 0]$.

Turning attention to Figure 5.3(b), in terms of ES risk, all strategies behave similarly to the left of $ES \simeq 0$. However, the EW-ES efficient frontier continues to generate positive ES for $EW < 50$. Essentially, this is because the EW-ES strategy focuses on maximizing ES, but at the expense of giving up increases in $Prob[W_T > 0]$. Recall from our previous discussion that the EW-PS and EW-LS strategies only make sense if we look at points to the left of the *knee* of the curves.

From a practical point of view, it is not clear that maximizing ES when it is positive is consistent with the retiree's view of risk (i.e. running out of savings).

5.8 Tests for robustness: bootstrap resampling

We compute and store the optimal controls for EW-PS, EW-LS and EW-ES objective functions, based on the parametric market model described in Appendix A. We then test these controls using block bootstrap resampling of the market data in 1926:1-2023:12 (Politis and Romano, 1994; Politis and White, 2004; Patton et al., 2009; Cogneau and Zakalmouline, 2013; Dichtl et al., 2016; Cavaglia et al., 2022; Simonian and Martirosyan, 2022; Anarkulova et al., 2022).

Figure 5.4 compares the synthetic market results (test and train on the parametric market model) as well as testing this control on bootstrapped historical data, for all three objective functions: EW-LS, EW-PS and EW-ES. The bootstrapped tests are carried out for a range of expected blocksizes. In all cases, for all blocksizes, the efficient frontiers are quite close, indicating that the controls computed using the parametric market model in Appendix A are robust to model misspecification.

Further insight can be obtained by examining the summary statistics in Table 5.3 (synthetic market) and Table 5.4 (historical market). It would seem that the EW-LS strategy is a good compromise, having a relatively small $Prob[W_T < 0]$, and with an expected shortfall close to the optimal value from the EW-ES solution. Note that $\mathbb{W}$ is a byproduct of the optimization algorithm for the EW-ES problem. This may not correspond, intuitively, to the investor's preferences. For example, as move rightward along the EW-ES efficient frontier, $\mathbb{W}$ becomes a large positive value. Any value of W_T to the left of this point, is regarded (by the objective function) as a bad outcome, which probably does not correspond to most investor's concept of risk.

In contrast, $\mathbb{W}$ is an input parameter for EW-PS and EW-LS. In our case, since our main concern is running out of cash, setting $\mathbb{W} = 0$ is clearly a reasonable choice.

Note that Table 5.4 shows that the ES(5%) result for the EW-LS control (computed in the synthetic market) is actually better than for the EW-ES control (also computed in the synthetic market) control, when tested in the historical market. This suggests that the EW-LS control is more robust than the EW-ES control.

Strategy	κ	$E[\sum_i \mathfrak{q}_i]/M$	LS($\mathbb{W} = 0$)	ES(5%)	$Prob[W_T < 0]$	$\mathbb{W}$
EW-ES	0.5925	52.97	-11.106	-102.36	.271	-31.15
EW-LS	9.3822	52.99	-5.3332	-106.66	.048	0.0
EW-PS	2670.9	53.04	-9.2747	-185.40	.027	0.0

TABLE 5.3: *Synthetic market, summary statistics for EW-PS, EW-LS, and EW-ES objective functions, EW $\simeq$ 53 for all strategies. LS refers to $E[\min(W_T - \mathbb{W}, 0)]$, ES(5%) is the mean of the worst five per cent of the outcomes. $\mathbb{W}$ is specified for EW-PS and EW-LS, while it is an outcome of the EW-ES optimization. Scenario in Table 5.2. Parameters in Table A.1. Units: thousands of dollars (real). M is the total number of withdrawals (rebalancing dates).*

Strategy	$E[\sum_i \mathfrak{q}_i]/M$	LS($\mathbb{W} = 0$)	ES(5%)	$Prob[W_T < 0]$
EW-ES	53.18	-5.4192	-46.21	0.250
EW-LS	52.93	-1.5448	-30.85	0.0226
EW-PS	53.12	-3.705	-74.02	0.0120

TABLE 5.4: *Block bootstrap resampling, summary statistics for EW-PS, EW-LS, and EW-ES objective functions, EW $\simeq$ 53 for all strategies. Blocksize two years, 10^6 bootstrap resamples. Optimal controls computed in the synthetic market. LS refers to $E[\min(W_T - \mathbb{W}, 0)]$, ES(5%) is the mean of the worst five per cent of the outcomes. Scenario in Table 5.2. Parameters in Table A.1. Units: thousands of dollars (real). M is the total number of withdrawals (rebalancing dates).*

Another test of robustness is shown in Table 5.5. Here, we rank each strategy, in terms of performance, according to each risk criteria, in the historical market. All strategies have approximately the same $EW \simeq 53$. In this case, we can see that EW-LS is the clear winner.

5.9 Comparison with the Bengen strategy

Consider Figure 5.4(a), with EW $\simeq$ 50. This translates to average withdrawals of 5% of initial wealth with $Prob[W_T < 0] < 1\%$. Contrast this with the bootstrapped results for the Bengen strategy, where the withdrawals are 40 per year (4% of initial wealth (real)), with a probability of failure $> 10\%$.

Strategy	Rank			
	LS($\mathbb{W} = 0$)	ES(5%)	$Prob[W_T < 0]$	Total Score
EW-ES	3	2	3	8
EW-LS	1	1	2	4
EW-PS	2	3	1	6

Table 5.5: *Ranking of strategies, historical market. Each strategy is ranked (first, second or third). Optimal controls computed in the synthetic market. Total score is the sum of the rows, smaller is better. EW $\simeq$ 53 for all strategies. Data is from Table 5.4. Block bootstrap resampling, summary statistics for EW-PS, EW-LS, and EW-ES objective functions. Blocksize two years, 10^6 bootstrap resamples. LS refers to $E[\min(W_T - \mathbb{W}, 0)]$, ES(5%) is the mean of the worst five per cent of the outcomes. Scenario in Table 5.2. Parameters in Table A.1. Units: thousands of dollars (real).*

Similarly, Figure 5.4(b) has (EW,ES) = (50,0) for the EW-ES optimal strategy, compared with (EW,ES) = $\simeq$ (40, -350) for the Bengen strategy.

Finally, Figure 5.4(c) gives (EW,LS) = (50,0) for the EW-LS optimal policy, compared with (EW,LS) = $\simeq$ (40, -20) for the Bengen strategy.

Of course, all these comparisons come with the caveat that the Bengen strategy withdraws a fixed amount per year, while the results for the optimal strategies are in terms of expected withdrawals.

6 CDFs of the optimal strategies

Figure 6.1 shows the CDF curves for the final wealth W_T for all three strategies. The results are shown for both the synthetic and historical market. For each strategy, the point on the efficient frontier was selected so that $EW \simeq 53$. It is interesting to observe that all strategies have similar CDFs for $X > 0$ ($Prob[W_T > 0]$), and rapidly increase to the right of this point. This indicates that all strategies are efficient in the sense that there is little unspent wealth at $t = 30$ years (age 95). This contrasts with the Bengen policy, which has a non-trivial probability of either running out of cash or ending up with large unspent wealth.

Figure 6.2(b) focuses on the area of the CDF curves near $X = 0$. Examining the synthetic market results, Figure 6.2(a), we can see that the EW-PS and EW-LS curves behave very similarly near $W_T = 0$, but there is a difference in the left tail, as might be expected. We can see that EW-PS does an excellent job of producing small $Prob[W_T < 0]$. However, this strategy does not do well in the left tail compared with EW-LS. The EW-ES strategy, on the other hand, has a fairly high probability that $W_T < 0$, compared with either EW-PS or EW-LS. However, this is a bit misleading, since the EW-ES CDF plots below the other strategies for $X < -40$. The historical market CDFs, Figure 6.2(b), are qualitatively similar to the synthetic market curves.

7 Comments on EW-LS, EW-PS and EW-ES strategies

The EW-PS optimal control, using PS risk (probability of running out of savings), seems at first sight to be an appealing intuitive strategy. However, the CDF of the final wealth shows that this strategy generates a very fat left tail. This is simply due to the fact that PS risk does not weight the amounts less than $\mathbb{W}$.

The EW-ES optimal control also has a simple intuitive interpretation. The ES (mean of the worst 5% of the outcomes) is a dollar amount that can be compared with, for example, the retiree's

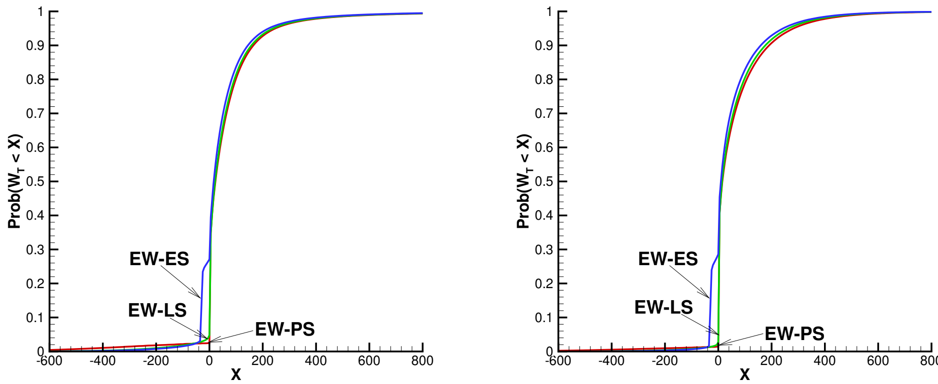

(a) *CDF curves, synthetic market*

(b) *CDF curves, bootstrapped historical market.*

FIGURE 6.1: *CDF curves, all strategies have the same average EW $\simeq$ 53. Optimal controls computed using the synthetic market model. Tests in the synthetic market Figure 6.1(a) and the historical market, Figure 6.1(b) shown. Expected blocksize: two years. Real stock index: deflated real capitalization weighted CRSP, real bond index: deflated 30 day T-bills. Scenario in Table 5.2. Parameters in Table A.1.*

real estate hedge of last resort. However, in some cases, the ES can be large and positive, which does not correspond to what we would normally think of as risk. In addition, EW-ES is formally time inconsistent. There is, of course, an induced time consistent policy, which is simply the EW-LS control with suitable $\mathbb{W}$.

The EW-LS control is trivially time-consistent. The investor specified parameter $\mathbb{W}$ in the EW-LS objective function is easily interpreted as the disaster level of final wealth. The EW-LS controls also perform reasonably well using ES (expected shortfall) or PS (probability of shortfall) as risk measures. The EW-LS control is also more robust, when tested in the historical (bootstrapped) market, compared to the other strategies.

Consequently, we recommend use of the EW-LS control for decumulation.

8 Detailed results: EW-LS, historical market

Figure 8.1(a) shows the percentiles of the optimal fraction in stocks, versus time, in the historical market. Initially, the fraction in stocks is a bit less than 0.60. The median fraction drops smoothly down to zero near year 29. At the fifth percentile, complete de-risking occurs at about year 16. In the case of poor investment returns, the allocation to stocks is 0.60-0.80 at the 95th percentile.

Figure 8.1(b) shows the wealth percentiles in the historical market. We can see that W_T just approaches zero at the 5th percentile, at year 29. Again, we remind the reader that it is assumed that the retiree has real estate which can be used to fund a shortfall at less than the 5th percentile. The expected shortfall at the 5% level in this case is about -30. Assuming that a reverse mortgage can be obtained for one half the value of the real estate, this suggests that real estate valued (in real terms) $>$ 60,000 can manage this risk.

Finally, we can see from Figure 8.1(c) that the median withdrawal rapidly increases to the maximum withdrawal by year one.

The heat maps for the optimal fraction in stocks and the optimal withdrawals are shown in Figure 8.2. Figure 8.2(b) shows that the withdrawal control is approximately bang-bang, i.e. it is

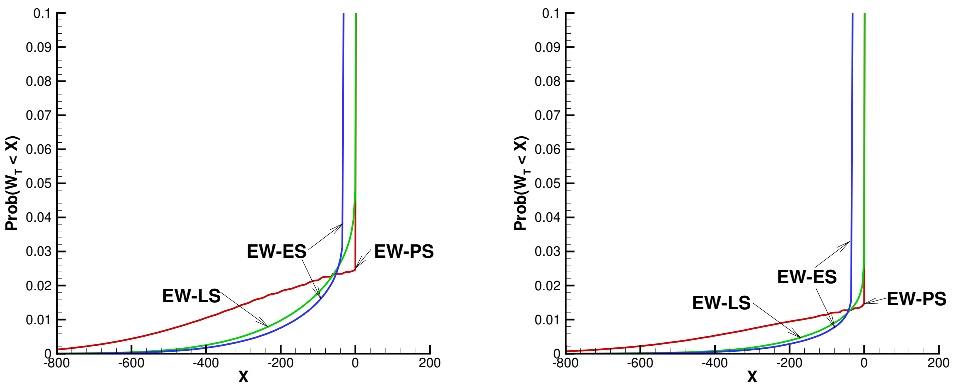

(a) *CDF curves, synthetic market*

(b) *CDF curves, bootstrapped historical market. 10^6 bootstrap resamples.*

FIGURE 6.2: *Zoomed plots, CDF curves, all strategies have the same average EW $\simeq$ 53. Optimal controls computed using the synthetic market model. Tests in the synthetic market Figure 6.1(a) and the historical market, Figure 6.1(b) shown. Expected blocksize: two years. Real stock index: deflated real capitalization weighted CRSP, real bond index: deflated 30 day T-bills. Scenario in Table 5.2. Parameters in Table A.1.*

only ever optimal to withdraw $\mathfrak{q}_{\max}$ or $\mathfrak{q}_{\min}$ and nothing in between. For an explanation of this, see Forsyth (2022).

9 Conclusions

As noted in Anarkulova et al. (2023), retirees and wealth advisors demonstrate a revealed preference for spending rules for decumulation of DC pension plans. Almost all previous work on spending rules postulates heuristic strategies and tests these rules using historical data.

We follow a different methodology here. We determine the spending rules as the solution of an optimal stochastic control problem. The control problem is solved numerically, based on a parametric model of long term stock and bond returns.

For an optimal control problem, the first order of business is to specify the objective function, in terms of risk and reward. Since we allow variable withdrawals (subject to maximum and minimum constraints) we define reward as the total expected (real) withdrawals over a 30 year retirement (EW).

We assess and compare ES, LS, and PS risk measures. We establish mathematically that, under certain assumptions, the set of optimal controls associated with all expected reward and expected shortfall (EW-ES) Pareto efficient frontier curves is identical to the set of optimal controls for all expected reward and linear shortfall (EW-LS) Pareto efficient frontier curves. This has the consequence that the set of optimal controls for EW-ES$_{t_0}$ are time consistent under the EW-LS$_{t_0}$ risk measure.

Based on our analysis and computational assessment of various risk measures, we conclude that risk as measured by linear shortfall LS, i.e. linearly weighting the final wealth below zero, is an appropriate risk measure.

As noted, the optimal EW-LS control is computed using a parametric market model. However, this control has been tested out-of-sample using block bootstrap resampling of historical data. These tests show that the optimal control is robust to parameter misspecification.

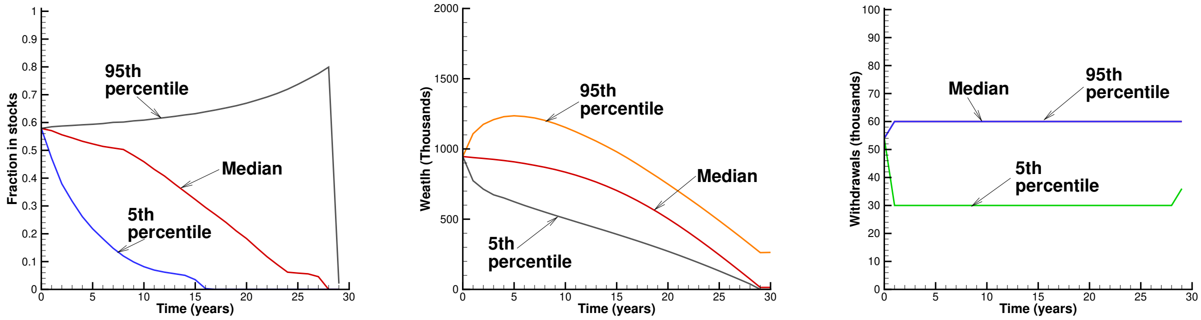

(a) *Percentiles fraction in stocks* (b) *Percentiles wealth* (c) *Percentiles withdrawals*

FIGURE 8.1: *Scenario in Table 5.2. EW-LS control computed from problem EW-LS Problem (4.4). Parameters based on the real CRSP index, and real 30-day T-bills (see Table A.1). Control computed and stored from the Problem (4.4) in the synthetic market. Control used in the historical market,* 10^6 *bootstrap samples.* $q_{min} = 30, q_{\max} = 60$ *(per year), EW* $\simeq 53.0$*. Units: thousands of dollars. Expected blocksize two years.*

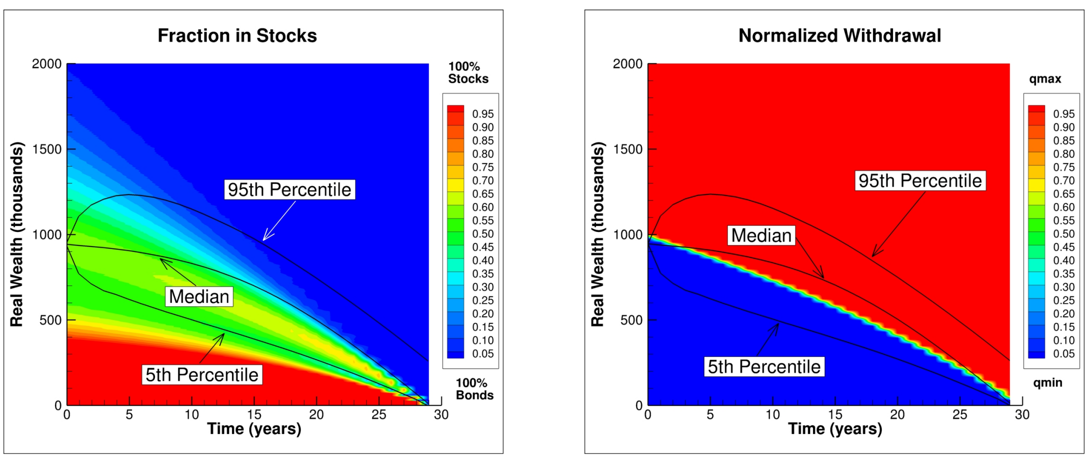

(a) *Fraction in stocks* (b) *Withdrawals*

FIGURE 8.2: *Optimal EW-LS. Heat map of controls: fraction in stocks and withdrawals, computed from Problem EW-LS (4.4). Real capitalization weighted CRSP index, and real 30-day T-bills. Scenario given in Table 5.2. Control computed and stored from the Problem 4.4 in the synthetic market.* $q_{min} = 30, q_{\max} = 60$ *(per year). EW* $\simeq 53.0$*. Percentiles from bootstrapped historical market. Normalized withdrawal* $(q - q_{\min})/(q_{\max} - q_{\min})$*. Units: thousands of dollars.*

Bootstrap resampling of historical data shows that the 4% rule (initial capital: one million, withdrawing 4% real of initial capital per year) has a probability of failure $> 10\%$, and expected shortfall ES(5%) $< -\$350{,}000$. In contrast, under bootstrap resampling tests, the EW-LS optimal control can withdraw 5% of initial wealth annually, on average, (adjusted for inflation) with a 98% probability of success, with an ES(5%) $\simeq -\$15{,}000$.

The EW-LS controls are dynamic. Both withdrawal amounts and stock allocation depend on the realized portfolio wealth (and time to go). However, the controls are summarized as easy to interpret heat maps, which makes implementation of these optimal controls straightforward.

Finally, we note that the optimal controls can be computed directly from the bootstrapped resampled data, without specifying a parametric model of the underlying stock and bond processes.

This requires use of machine learning techniques (Ni et al., 2022; van Staden et al., 2023; 2025). These methods also allow use of more assets in terms of investment choices. We leave further study of machine learning techniques in the context of DC decumulation for future work.

10 Acknowledgements

Forsyth's work was supported by the Natural Sciences and Engineering Research Council of Canada (NSERC) grant RGPIN-2017-03760. Li's work was supported by a Natural Sciences and Engineering Research Council of Canada (NSERC) grant RGPIN-2020-04331.

11 Declaration

The authors have no conflicts of interest to report.

Appendix

A Parametric Model

We assume that the investor has access to two funds: a broad market stock index fund and a constant maturity bond index fund. The investment horizon is T. Let S_t and B_t respectively denote the real (inflation adjusted) *amounts* invested in the stock index and the bond index respectively. In general, these amounts will depend on the investor's strategy over time, as well as changes in the real unit prices of the assets. In the absence of an investor determined control (i.e. cash withdrawals or rebalancing), all changes in S_t and B_t result from changes in asset prices. We model the stock index as following a jump diffusion.

In addition, we follow the usual practitioner approach and directly model the returns of the constant maturity bond index as a stochastic process (see, e.g. Lin et al., 2015; MacMinn et al., 2014). As in MacMinn et al. (2014), we assume that the constant maturity bond index follows a jump diffusion process. Empirical justification for this can be found in Forsyth et al. (2022), Appendix A.

Let $S_{t^-} = S(t-\epsilon), \epsilon \to 0^+$, i.e. t^- is the instant of time before t, and let ξ^s be a random number representing a jump multiplier. When a jump occurs, $S_t = \xi^s S_{t^-}$. Allowing for jumps permits modelling of non-normal asset returns. We assume that $\log(\xi^s)$ follows a double exponential distribution (Kou, 2002; Kou and Wang, 2004). If a jump occurs, u^s is the probability of an upward jump, while $1-u^s$ is the chance of a downward jump. The density function for $y = \log(\xi^s)$ is

$$f^s(y) = u^s \eta_1^s e^{-\eta_1^s y} \mathbf{1}_{y \geq 0} + (1-u^s)\eta_2^s e^{\eta_2^s y} \mathbf{1}_{y<0} \ . \tag{A.1}$$

We also define

$$\gamma_\xi^s = E[\xi^s - 1] = \frac{u^s \eta_1^s}{\eta_1^s - 1} + \frac{(1-u^s)\eta_2^s}{\eta_2^s + 1} - 1 \ . \tag{A.2}$$

In the absence of control, S_t evolves according to

$$\frac{dS_t}{S_{t^-}} = \left(\mu^s - \lambda_\xi^s \gamma_\xi^s\right)\, dt + \sigma^s\, dZ^s + d\left(\sum_{i=1}^{\pi_t^s} (\xi_i^s - 1)\right) , \tag{A.3}$$

where μ^s is the (uncompensated) drift rate, σ^s is the volatility, dZ^s is the increment of a Wiener process, π_t^s is a Poisson process with positive intensity parameter λ_ξ^s, and ξ_i^s are i.i.d. positive random variables having distribution (A.1). Moreover, ξ_i^s, π_t^s, and Z^s are assumed to all be mutually independent.

Similarly, let the amount in the bond index be $B_{t^-} = B(t-\epsilon), \epsilon \to 0^+$. In the absence of control, B_t evolves as

$$\frac{dB_t}{B_{t^-}} = \left(\mu^b - \lambda_\xi^b \gamma_\xi^b + \mu_c^b \mathbf{1}_{\{B_{t^-}<0\}}\right) dt + \sigma^b\, dZ^b + d\left(\sum_{i=1}^{\pi_t^b} (\xi_i^b - 1)\right), \tag{A.4}$$

where the terms in equation (A.4) are defined analogously to equation (A.3). In particular, π_t^b is a Poisson process with positive intensity parameter λ_ξ^b, and ξ_i^b has distribution

$$f^b(y = \log \xi^b) = u^b \eta_1^b e^{-\eta_1^b y} \mathbf{1}_{y \geq 0} + (1 - u^b) \eta_2^b e^{\eta_2^b y} \mathbf{1}_{y<0}\ , \tag{A.5}$$

and $\gamma_\xi^b = E[\xi^b - 1]$. ξ_i^b, π_t^b, and Z^b are assumed to all be mutually independent. The term $\mu_c^b \mathbf{1}_{\{B_{t^-}<0\}}$ in equation (A.4) represents the extra cost of borrowing (the spread).

The diffusion processes are correlated, i.e. $dZ^s \cdot dZ^b = \rho_{sb}\, dt$. The stock and bond jump processes are assumed mutually independent. See Forsyth (2020b) for justification of the assumption of stock-bond jump independence.

We use the threshold technique (Mancini, 2009; Cont and Mancini, 2011; Dang and Forsyth, 2016) to estimate the parameters for the parametric stochastic process models. Since the index data is in real terms, all parameters reflect real returns. Table A.1 shows the results of calibrating the models to the historical data. The correlation ρ_{sb} is computed by removing any returns which occur at times corresponding to jumps in either series, and then using the sample covariance. Further discussion of the validity of assuming that the stock and bond jumps are independent is given in Forsyth (2020b).

CRSP	μ^s	σ^s	λ^s	u^s	η_1^s	η_2^s	ρ_{sb}
	0.087323	0.147716	0.316326	0.225806	4.3591	5.53370	0.095933
30-day T-bill	μ^b	σ^b	λ^b	u^b	η_1^b	η_2^b	ρ_{sb}
	0.0032	0.0140	0.3878	0.3947	61.5350	53.4043	0.095933

Table A.1: *Parameters for parametric market models (A.3 and (A.4, fit to CRSP data (inflation adjusted) for 1926:1-2023:12.*

B Numerical Techniques

We solve problems (4.4) using the techniques described in detail in Forsyth and Labahn (2019); Forsyth (2020a; 2022). We give only a brief overview here.

We localize the infinite domain to $(s,b) \in [s_{\min}, s_{\max}] \times [b_{\min}, b_{\max}]$, and discretize $[b_{\min}, b_{\max}]$ using an equally spaced $\log b$ grid, with n_b nodes. Similarly, we discretize $[s_{\min}, s_{\max}]$ on an equally spaced $\log s$ grid, with n_s nodes. For case $b < 0$, we define a reflected grid $b' = -b$, with the $n_b \times n_s$ nodes. This represents the insolvent case nodes. The PIDE for $b' > 0$ has the same form as for

$b > 0$. This idea can be used more generally if leverage is permitted, which we do not explore in this work. Localization errors are minimized using the domain extension method in Forsyth and Labahn (2019).

At rebalancing dates, we solve the local optimization problem by discretizing $(\mathfrak{q}(\cdot), \mathfrak{p}(\cdot))$ and using exhaustive search. Between rebalancing dates, we solve a two dimensional partial integro-differential equation (PIDE) using Fourier methods (Forsyth and Labahn, 2019; Forsyth, 2022). Finally, in the case of EW-ES, the outer optimization over $\mathbb{W}$ is solved using a one-dimensional method.

We used the value $\epsilon = -10^{-4}$ in equation (4.4), which forces the investment strategy to be bond heavy if the remaining wealth in the investor's account is large, and $t \to T$. Using this small value of gave the same results as $\epsilon = 0$ for the summary statistics, to four digits. This is simply because the states with very large wealth have low probability. However, this stabilization procedure produced smoother heat maps for large wealth values, without altering the summary statistics appreciably.

B.1 Convergence Test: Synthetic Market

Table B.1 shows a detailed convergence test for the base case problem given in Table 5.2, for the EW-ES problem. The results are given for a sequence of grid sizes, for the dynamic programming algorithm in (Forsyth, 2022) and Appendix B. The dynamic programming algorithm appears to converge at roughly a second order rate. The optimal control computed using dynamic programming is stored, and then used in Monte Carlo computations. The Monte Carlo results are in good agreement with the dynamic programming solution. For all the numerical examples, we will use the 2048×2048 grid, since this seems to be accurate enough for our purposes.

	Algorithm in (Forsyth, 2022) and Appendix B			Monte Carlo	
Grid	LS	$E[\sum_i \mathfrak{q}_i]/M$	Value Function	LS	$E[\sum_i \mathfrak{q}_i]/M$
512×512	-1.40884	50.9082	1484.981	-1.26443	50.938
1024×1024	-1.32050	50.9491	1488.864	-1.27396	50.953
2048×2048	-1.30148	50.9643	1489.880	-1.28189	50.963

Table B.1: *EW-LS convergence test. Real stock index: deflated real capitalization weighted CRSP, real bond index: deflated 30 day T-bills. Scenario in Table 5.2. Parameters in Table A.1. The Monte Carlo method used* 2.56×10^6 *simulations. The MC method used the control from the solving the PIDEs as described in Appendix B.* $\kappa = 30, \mathbb{W} = 0.0$. *Grid refers to the grid used in the Algorithm in Appendix B:* $n_x \times n_b$, *where* n_x *is the number of nodes in the* $\log s$ *direction, and* n_b *is the number of nodes in the* $\log b$ *direction. Units: thousands of dollars (real).* M *is the total number of withdrawals (rebalancing dates).*

C Effect of Stabilization term

Recall that the optimization problem, for all objective functions, becomes ill-posed along any path where $W_t \gg \mathbb{W}$, $t \to T$. To remove this problem, the stabilization term

$$\epsilon E[W_T] \tag{C.1}$$

is added to each objective function. We set $|\epsilon| \ll 1$, to ensure that this term has little effect unless we are in the ill-posed region. Essentially, if $\epsilon < 0$, then this forces the portfolio to invest 100% in

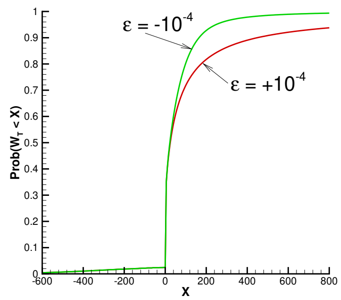

Figure C.1: *EW-PS CDF of the terminal wealth, with stabilization parameters shown. Point on curve where EW $\simeq$ 53.0. Real stock index: deflated real capitalization weighted CRSP, real bond index: deflated 30 day T-bills. Scenario in Table 5.2. Parameters in Table A.1. Synthetic market.*

bonds. On the other hand, if $\epsilon > 0$, then the portfolio will invest 100% in stocks. We remark here that these choices are essentially arbitrary: by assumption, the 95-year old retiree has a short life expectancy, and has large wealth, so that even with maximum withdrawals, there is almost zero probability of running out of cash.

To verify that the choice of positive or negative ϵ has little effect near $W_t = \mathbb{W}$, Figure C.1 shows the CDF curves for the EW-PS strategy (EW = 53.0), for both positive and negative ϵ. We can see that both curves overlap for $W_T \leq 100$. Consequently, left tail risk measures will be identical for both cases, and there will be no differences in average withdrawals, since we will be constrained by the maximum withdrawal specification. To the right of $W_T = 100$, we can see that for $\epsilon > 0$, there is higher probability of obtaining larger W_T compared to the case $\epsilon < 0$. This is of course expected, since investing in all stocks, (when W_t is large) will have a larger expected portfolio value.

The CDF curves for $\pm\epsilon$ for EW-ES and EW-LS policies are similar.

References

Ackerly, A., N. N, and D. Nikles (2021). To spend or not to spend? BlackRock white paper, `https://www.blackrock.com/us/individual/literature/whitepaper/spending-retirement-assets-final-whitepaper.pdf`.

Anarkulova, A., S. Cederburg, and M. S. O'Doherty (2022). Stocks for the long run? Evidence from a broad sample of developed markets. *Journal of Financial Economics 143:1*, 409–433.

Anarkulova, A., S. Cederburg, M. S. O'Doherty, and R. W. Sias (2023). The safe withdrawal rate: Evidence from a broad sample of developed markets. SSRN 4227132.

Bannerje, S. (2021). Decoding retiree spending. R. Rowe Price Insights on Retirement, `https://www.troweprice.com/institutional/us/en/insights/articles/2021/q1/decoding-retiree-spending-na.html`.

Bengen, W. (1994). Determining withdrawal rates using historical data. *Journal of Financial Planning 7*, 171–180.

Bernhardt, T. and C. Donnelly (2018). Pension decumulation strategies: A state of the art report. Technical Report, Risk Insight Lab, Heriot Watt University.

Bjork, T., M. Khapko, and A. Murgoci (2021). *Time inconsistent control theory with finance applications*. New York: Springer Finance.

Bjork, T. and A. Murgoci (2010). A general theory of Markovian time inconsistent stochastic control problems. SSRN 1694759.

Bjork, T. and A. Murgoci (2014). A theory of Markovian time inconsisent stochastic control in discrete time. *Finance and Stochastics 18*, 545–592.

Browning, C., R. Guo, Y. Cheng, and M. S. Finke (2016). Spending in retirement: determining the consumption gap. *Journal of Financial Planning 26(2)*, 42–53.

Cavaglia, S., L. Scott, K. Blay, and S. Hixon (2022). Multi-asset class factor premia: A strategic asset allocation perspective. *The Journal of Portfolio Management 48:9*, 14–32.

Chen, M., M. Shirazi, P. A. Forsyth, and Y. Li (2023). Machine learning and hamilton-jacobi-bellman equation for optimal decumulation: a comparison study. Working paper, Cheriton School of Computer Science, `https://cs.uwaterloo.ca/~paforsyt/benchmarkNNpaper.pdf`.

Cogneau, P. and V. Zakalmouline (2013). Block bootstrap methods and the choice of stocks for the long run. *Quantitative Finance 13*, 1443–1457.

Cont, R. and C. Mancini (2011). Nonparametric tests for pathwise properties of semimartingales. *Bernoulli 17*, 781–813.

Dang, D.-M. and P. A. Forsyth (2014). Continuous time mean-variance optimal portfolio allocation under jump diffusion: a numerical impulse control approach. *Numerical Methods for Partial Differential Equations 30*, 664–698.

Dang, D.-M. and P. A. Forsyth (2016). Better than pre-commitment mean-variance portfolio allocation strategies: a semi-self-financing Hamilton-Jacobi-Bellman equation approach. *European Journal of Operational Research 250*, 827–841.

Dichtl, H., W. Drobetz, and M. Wambach (2016). Testing rebalancing strategies for stock-bond portfolios across different asset allocations. *Applied Economics 48*, 772–788.

Forsyth, P. and G. Labahn (2019). $\epsilon-$Monotone Fourier methods for optimal stochastic control in finance. *Journal of Computational Finance 22:4*, 25–71.

Forsyth, P., K. Vetzal, and G. Westmacott (2024). Optimal performance of a tontine overlay subject to withdrawal constraints. *ASTIN Bulletin 54:1*, 94–128.

Forsyth, P. A. (2020a). Multi-period mean CVAR asset allocation: Is it advantageous to be time consistent? *SIAM Journal on Financial Mathematics 11:2*, 358–384.

Forsyth, P. A. (2020b). Optimal dynamic asset allocation for DC plan accumulation/decumulation: Ambition-CVAR. *Insurance: Mathematics and Economics 93*, 230–245.

Forsyth, P. A. (2022). A stochastic control approach to defined contribution plan decumulation: The nastiest, hardest problem in finance. *North American Actuarial Journal 26:2*, 227–251.

Forsyth, P. A. and K. R. Vetzal (2019). Optimal asset allocation for retirement savings: deterministic vs. time consistent adaptive strategies. *Applied Mathematical Finance 26:1*, 1–37.

Forsyth, P. A., K. R. Vetzal, and G. Westmacott (2022). Optimal control of the decumulation of a retirement portfolio with variable spending and dynamic asset allocation. *ASTIN Bulletin 51:3*, 905–938.

Fullmer, R. K. (2019). Tontines: a pracitioner's guide to mortality-pooled investments. CFA Institute Research Foundation `https://www.cfainstitute.org/en/research/foundation/2019/tontines`.

Guyton, J. T. and W. J. Klinger (2006). Decision rules and maximum initial withdrawal rates. *Journal of Financial Planning 19*(3), 48–58.

Hamilton, M. (2001, December). The Financial Circumstances of Elderly Canadians and the Implications for the Design of Canada's Retirement Income System. In P. Grady and A. Sharpe (Eds.), *The State of Economics in Canada: Festschrift in Honour of David Slater*, The State of Economics in Canada: Festschrift in Honour of David Slater, pp. 225–253. Centre for the Study of Living Standards.

Hatch, J. E. and R. W. White (1985). Canadian stocks, bonds, bills and inflation: 1950-1983. Financial Analysts Research Foundation Mongraph Series, Number 19.

Hill, C. (2016). Older people fear this more than death. `https://www.marketwatch.com/story/older-people-fear-this-more-than-death-2016-07-18`.

Irlam, G. (2014). Portfolio size matters. *Journal of Personal Finance 13*(2), 9–16.

Kou, S. G. (2002). A jump-diffusion model for option pricing. *Management Science 48*, 1086–1101.

Kou, S. G. and H. Wang (2004). Option pricing under a double exponential jump diffusion model. *Management Science 50*, 1178–1192.

Lin, Y., R. MacMinn, and R. Tian (2015). De-risking defined benefit plans. *Insurance: Mathematics and Economics 63*, 52–65.

MacDonald, B.-J., B. Jones, R. J. Morrison, R. L. Brown, and M. Hardy (2013). Research and reality: A literature review on drawing down retirement financial savings. *North American Actuarial Journal 17*, 181–215.

MacMinn, R., P. Brockett, J. Wang, Y. Lin, and R. Tian (2014). The securitization of longevity risk and its implications for retirement security. In O. S. Mitchell, R. Maurer, and P. B. Hammond (Eds.), *Recreating Sustainable Retirement*, pp. 134–160. Oxford: Oxford University Press.

Mancini, C. (2009). Non-parametric threshold estimation models with stochastic diffusion coefficient and jumps. *Scandinavian Journal of Statistics 36*, 270–296.

Ni, C., Y. Li, P. A. Forsyth, and R. Caroll (2022). Optimal asset allocation for outperforming a stochastic benchmark. *Quantitative Finance 22(9)*, 1595–1626.

Patton, A., D. Politis, and H. White (2009). Correction to: automatic block-length selection for the dependent bootstrap. *Econometric Reviews 28*, 372–375.

Peijnenburg, K., T. Nijman, and B. J. Werker (2016). The annuity puzzle remains a puzzle. *Journal of Economic Dynamics and Control 70*, 18–35.

Pfeiffer, S., J. R. Salter, and H. E. Evensky (2013). Increasing the sustainable withdrawal rate using the standby reverse mortgage. *Journal of Financial Planning 26:12*, 55–62.

Politis, D. and J. Romano (1994). The stationary bootstrap. *Journal of the American Statistical Association 89*, 1303–1313.

Politis, D. and H. White (2004). Automatic block-length selection for the dependent bootstrap. *Econometric Reviews 23*, 53–70.

Powell, W. (2025). On state variables. https://castle.princeton.edu/statevariables/.

Rappaport, A. (2019). Insights on spending and asset management in retirement. SOA report, https://www.soa.org/499c88/globalassets/assets/files/resources/research-report/2019/2019-spending-asset-management-report.pdf.

Ritholz, B. (2017). Tackling the 'nastiest, hardest problem in finance'. www.bloomberg.com/view/articles/2017-06-05/tackling-the-nastiest-hardest-problem-in-finance.

Rockafellar, R. T. and S. Uryasev (2000). Optimization of conditional value-at-risk. *Journal of Risk 2*, 21–42.

Shefrin, H. M. and R. H. Thaler (1988). The behavioral life-cycle hypothesis. *Economic Inquiry 26*, 609–643.

Simonian, J. and A. Martirosyan (2022). Sharpe parity redux. *The Journal of Portfolio Management 48:9*, 183–193.

Strub, M., D. Li, X. Cui, and J. Gao (2019). Discrete-time mean-CVaR portfolio selection and time-consistency induced term structure of the CVaR. *Journal of Economic Dynamics and Control 108*. Article 103751 (electronic).

Thinking Ahead Institute (2024). Global pension assets study 2024. https://www.thinkingaheadinstitute.org/content/uploads/2024/02/GPAS-2024.pdf.

van Staden, P., P. Forsyth, and Y. Li (2023). Beating a benchmark: dynamic programming may not be the right numerical approach. *SIAM Journal on Financial Mathematics 14:2*, 407–451.

van Staden, P. M., D.-M. Dang, and P. Forsyth (2021). The surprising robustness of dynamic mean-variance portfolio optimization to model misspecification errors. *European Journal of Operational Research 289:2*, 74–792.

van Staden, P. M., P. A. Forsyth, and Y. Li (2025). A global-in-time neural network approach to dynamic portfolio optimization. to appear, Applied Mathematical Finance.

Vigna, E. (2014). On efficiency of mean-variance based portfolio selection in defined contribution pension schemes. *Quantitative Finance 14*, 237–258.

Vigna, E. (2017). Tail optimality and preferences consistency for intertemporal optimization problems. Working paper no. 502 , Collegio Carlo Alberto, Università Degli Studi di Torino.

Weinert, J.-H. and H. Gründl (2021). The modern tontine: an innovative instrument for longevity risk management in an aging society. *European Actuarial Journal 11*, 49–86.